MONTANA STATE UNIVERSITY

Fatigue behavior of glass fiber reinforced composite materials for wind turbine blades

by Rena Qiong Pan

A thesis submitted in partial fulfillment of the requirements for the degree of Master of Science in Chemical Engineering
Montana State University
© Copyright by Rena Qiong Pan (1994)

Abstract:
Glass fiber reinforced composite materials are used in a variety of applications such as wind turbine blades where resistance to fatigue (repeated loading and unloading) limits the service lifetime of the part. The fatigue process in these materials includes the gradual accumulation of stable damage prior to actual failure, with associated changes in material stiffness. In this thesis, a characterization of the cyclic. fatigue behavior of [0&deg/±45°]4 glass/polyester composite materials is presented in terms of the following parameters: static properties; S-N relationship; damage initiation and growth; fatigue modulus change; edge effects; and effects of triaxial reinforcement variations on fatigue properties.

The stiffness reductions resulting from fatigue damage were measured for laminates at various intervals during the cyclic life in order to determine changes in stiffness due to fatigue loading. The fatigue damage (matrix cracks, delamination and fiber breakage) was examined by edge replication and optical microscopy. Consistent with literature observations, the results suggest four distinct stages: undamaged, damage initiation and accumulation, crack interactions and delamination, and the final failure process.

Fatigue failure criteria have been examined for the same laminates. A secant modulus criterion was not found to be consistent with the data for this class of laminates. A cumulative secant modulus criterion was introduced. This criterion does appear to be valid for the limited materials and load conditions tested in this thesis.

The effects of free (machined) test coupon edges on the fatigue resistance were investigated by conducting a series of tension-tension fatigue tests on two material systems. One system was a conventional laminate with machined edges, while the other was fabricated by wrapping the laminate edges during fabrication. The results show that edge effects on the fatigue resistance are not significant. The effects of triaxial reinforcement variations on the fatigue properties were also investigated. Of two cases studied, Material W with relatively loosely stitched structure performed significantly better under fatigue loading, consistent with expectations from finite element modelling. No significant effect of stitching on static strength was observed.

FATIGUE BEHAVIOR OF GLASS FIBER REINFORCED COMPOSITE MATERIALS FOR WIND TURBINE BLADES

BY

Rena Qiong Pan

A thesis submitted in partial fulfillment
of the requirements for the degree

of

Master of Science

in

Chemical Engineering

MONTANA STATE UNIVERSITY
Bozeman, Montana

April 1994

T1378
P1925

APPROVAL

of a thesis submitted by

Rena Qiong Pan

This thesis has been read by each member of the thesis committee and has been found to be satisfactory regarding content, English usage, format, citations, bibliographic style, and consistency, and is ready for submission to the College of Graduate Studies.

4/26/94 — Date

J. L. D. Mandell — Chairperson, Graduate Committee

Approved for the Major Department

4/27/94 — Date

John T. Sears — Head, Major Department

Approved for the College of Graduate Studies

5/16/94 — Date

R. L. Brown — Graduate Dean

STATEMENT OF PERMISSION TO USE

In presenting this thesis in partial fulfillment of the requirements for a master degree at Montana State University, I agree that the Library shall make it available to borrowers under rules of the library.

If I have indicated my intention to copyright this thesis (paper) by including a copyright notice page, copying is allowable only for scholarly purposes, consistent with "fair use" as prescribed in the U.S. Copyright Law. Requests for permission for extended quotation from or reproduction of this thesis (paper) in whole or in parts may be granted only by the copyright holder.

Signature Rena Q. Parr

Date 05/05/94

ACKNOWLEDGEMENTS

I wish to express my sincere appreciation to professor John F. Mandell for his supervision, advice and support through the course of this research. Thanks also are extended to professor John T. Sears and Professor Aleksandria Vinogradov for their kind suggestions, guidance and for serving on my committee.

I also wish to express my appreciation to several members of the Department of Chemical Engineering for their assistance. They are:

—Ms. Jane Curtis and Monica Hoey for helping me work out with the system.

—Mr. Lyman Fellows for his repeated willingness to assist me whenever called upon.

—Mr.Chuck Hedley and Dan Samborsky for their proofreading, constructive criticism and help.

—All my fellow graduate students and friends for their time and help.

—Sandia National Laboratories and National Renewable Energy Laboratory for their technical, financial, and material support of this study, through Subcontracts 40-8975 and XF-1-1109-5, respectively.

TABLE OF CONTENTS

Page

1. INTRODUCTION 1

2. BACKGROUND 3

Damage Development and Life Prediction 4
Overview 4
Literature Review 7

Delamination 19
Introduction 19
Literature Review 21

Introduction to This Study 25

3. EXPERIMENTAL TESTING PROGRAM 33

Tension-Tension Fatigue Tests..... 33

Materials 34

Specimen Preparation 35

Equipment and Test Procedure..... 36

Experimental Data Reduction 37

Damage Development Studies 39

Specimen Preparation..... 41

Replication Process and Crack Measurement 41

Optical Microscope System 42

4. RESULTS AND DISCUSSIONS 50

Fatigue Damage and Stiffness Changes 51

TABLE OF CONTENTS (CONTINUED)

	Page
Fatigue Failure Criteria	59
Edge Effects	62
Effect of Triaxial Reinforcing Fabric Variations	64
5. CONCLUSIONS AND RECOMMENDATIONS	96
Conclusions	96
Recommendations	99
REFERENCES	101
APPENDIXES	106
Table 1 - Characteristic's Mechanical properties	107
Table 2 - Crack density measurements on edge surface	108

LIST OF FIGURES

Figure		Page
1.	Specimen configuration	28
2.	Damage features in $[0/90/\pm45]_s$ laminate	29
3.	Laminate geometry and stress direction	30
4.	Fatigue secant modulus criterion	31
5.	Fatigue modulus criterion	32
6.	Lamina and laminate descriptions	44
7.	Wrapped laminate (Material W) geometry	45
8.	Tensile fatigue test coupon configuration	46
9.	Photograph of Instron 8501 Testing System	47
10.	Stress-time diagram in a fatigue test	48
11.	Microscope system	49
12.	The $[0°/\pm45°]_4$ fractured specimens	68
13.	Typical damage development for a $[0°/\pm45°]_4$ laminate	69
14.	Damage growth of triaxial laminates subjected cyclic loading at two load levels	70
15.	Edge replica from a $[0°/\pm45]_4$ laminate at Stage (I)	71
16(a)	Edge replica from a $[0°/\pm45]_4$ laminate at Stage (II)	72
16(b)	Schematic view of crack pattern	73

density as a function of cycles 76

20. Edge replica from a $[0°/\pm45]_4$ laminate at Stage (III) 77

21. Schematic diagram of local region of influence for matrix cracking and local delamination 78

22. Edge views showing a fiber break for 85 percent of expected life 79

23. Edge view showing a 45° fiber break at Stage (IV) .. 80

24. Change of elastic modulus during fatigue 81

25. Change of fatigue secant modulus during fatigue 82

26. *S-N* curve for Materials T and W 83

27. *S-N* curve for Materials U an V 84

28. Fracture surface of wrapped and unwrapped laminates tested at lower cyclic stresses 85

29(a) Stitching pattern for Material V 86

29(b) Stitching pattern for Material W 87

30. A cross-section view showing fiber distribution in Material W and V 88

31. Stress-strain curves for Materials V and W 90

32. *S-N* curves for Materials V and W 91

33. Stitching effects on fatigue damage growth and fatigue life for Materials V and W 92

34. Stitching effects on normalized fatigue damage growth for Materials V and W 93

35. Damage initiation from the stitching material..... 94

36. Stitching effects on fatigue fracture mode for Materials V and W 95

ABSTRACT

Glass fiber reinforced composite materials are used in a variety of applications such as wind turbine blades where resistance to fatigue (repeated loading and unloading) limits the service lifetime of the part. The fatigue process in these materials includes the gradual accumulation of stable damage prior to actual failure, with associated changes in material stiffness. In this thesis, a characterization of the cyclic fatigue behavior of $[0°/\pm45°]_4$ glass/polyester composite materials is presented in terms of the following parameters: static properties; *S-N* relationship; damage initiation and growth; fatigue modulus change; edge effects; and effects of triaxial reinforcement variations on fatigue properties.

The stiffness reductions resulting from fatigue damage were measured for laminates at various intervals during the cyclic life in order to determine changes in stiffness due to fatigue loading. The fatigue damage (matrix cracks, delamination and fiber breakage) was examined by edge replication and optical microscopy. Consistent with literature observations, the results suggest four distinct stages: undamaged, damage initiation and accumulation, crack interactions and delamination, and the final failure process.

Fatigue failure criteria have been examined for the same laminates. A secant modulus criterion was not found to be consistent with the data for this class of laminates. A cumulative secant modulus criterion was introduced. This criterion does appear to be valid for the limited materials and load conditions tested in this thesis.

The effects of free (machined) test coupon edges on the fatigue resistance were investigated by conducting a series of tension-tension fatigue tests on two material systems. One system was a conventional laminate with machined edges, while the other was fabricated by wrapping the laminate edges during fabrication. The results show that edge effects on the fatigue resistance are not significant. The effects of triaxial reinforcement variations on the fatigue properties were also investigated. Of two cases studied, Material W with relatively loosely stitched structure performed significantly better under fatigue loading, consistent with expectations from finite element modelling. No significant effect of stitching on static strength was observed.

CHAPTER ONE

INTRODUCTION

It is known that the cost of electricity from wind generation plants has been more expensive than that from other types of plants (*i.e.* coal and hydro-electric generation plants). In order to make wind energy more competitive and keep costs down, the wind industry has begun to design more efficient blades utilizing the high strength to weight ratio, less expensive, glass fiber reinforced composite materials. The fatigue resistance of wind turbine blade materials is an important design consideration since these wind turbine blades must withstand roughly forty million loading-unloading cycles each year, over their twenty to thirty year lifetime.

However, long-term fatigue data and models have not been adequately developed for the fiberglass composites from which wind turbine blades are constructed [1]. This is partly due to the focus during the past years on high performance carbon fiber epoxy composite materials by the aerospace industry which generates the majority of research on fatigue properties. The extreme fatigue resistance of carbon fibers limits the applicability of much of this work to wind turbine

limits the applicability of much of this work to wind turbine blades which use lower cost E-glass fibers. This general lack of mechanical property and mechanism data, as well as early design and fabrication problems with blades, has resulted in both widespread premature blade failures and inefficient overweight blades. Thus, the blades can be designed efficiently and safely, and the best materials can be selected and developed only through a better understanding and characterization of the basic long-term fatigue behavior and the mechanics of damage development for the particular materials of interest for blade applications.

Generation of the required basic material property data is typically performed through static and dynamic (cyclic) fatigue testing. Much of the previous research done in the area of glass reinforced polymers under fatigue was carried out only to lower and moderate numbers of cycles, typically up to one million. Thus, the objectives of this study are to establish the fundamental aspects of fatigue behavior, including fatigue failure criteria, damage mechanisms and fabrication effects. The latter include edge effects and effects of different reinforcement fabric types. Ultimately, the results may be used as design parameters and as a basis for materials selection. An understanding of the material behavior may lead to the development of improved low cost materials for fatigue dominated applications.

CHAPTER TWO

BACKGROUND

Fatigue properties of composite materials have been shown to depend on the type of the composite structure and constituents. Major constituents in fiber-reinforced composite material are the reinforcing fibers and the matrix. For economy of manufacture of thick sections the basic commercial form of continuous glass fibers is a strand, which is a collection of parallel filaments numbering 204 or more. These glass fibers are held together as stands by stitching materials (i.e. aramid and polyester), which is intended to maintain orientation of the individual fiber tows or to keep reinforcement plies together while handling. Benefits include better interlaminar shear properties, damage tolerance, and fiber alignment.

"Lamina" (ply) is formed by incorporating a large number of fibers into a thin layer of matrix. Laminated fibrous composites are made by bonding together two or more laminae. The individual unidirectional laminae or plies are oriented in such a manner that the resulting structural component has the desired mechanical and/or physical characteristics in

characteristics in different directions. Thus, one exploits the inherent anisotropy of fibrous composites to design a composite material having the appropriate properties.

The following section provides an overview of the literature on some important studies of damage development which are relevant to the work conducted during this study.

Damage Development and Life Prediction

Overview

Some of the major problems facing users of continuous fiber reinforced polymer matrix composites at the present time are related to the lack of understanding of the complex fatigue damage mechanisms that exist in these materials. It is not well established how accumulating fatigue damage affects the properties that govern structural response. Methods for detection and quantification of the damage also need development. Furthermore, there are few proven quantitative models that can be used to predict fatigue behavior for design purposes.

It is recognized that damage development in a composite is unlike the single dominant crack failure of a homogeneous, isotropic metallic or polymeric material subjected to cyclic loading, where fracture mechanics provides a theoretical concept for the analysis of fatigue crack growth and failure. In a composite material, fatigue damage and eventual failure

may occur from the initiation and propagation of a single crack, or may develop from a complex array of multiple cracks. The type of damage which develops depends on the type of material and loading. In either case, typical crack growth has been classified in three stages [2]: crack initiation, stable crack growth, and unstable crack growth. Eighty percent of fatigue life may be spent initiating a particular crack, where in other instances, particularly at high stresses, cracks may develop on the first loading cycle [3]. Most of the cracks in a composite never become unstable, but, instead propagate for same distance and then arrest, as at a ply boundary.

Damage in composite materials may consist of local delamination, ply failure, matrix cracking, fiber breakage, debonding, or complex combinations of these phenomena [4]. The fatigue damage mechanisms and resulting damage state will depend upon the material system (combination of fiber and matrix material), microstructure of arrangement, ply orientation and stacking sequence, loading history, component geometry, stress state and the quality of fabrication. Damage in a composite laminate is usually dispersed, irregular and does not propagate in a self-similar way. Therefore, even a precise quantitative prediction of crack growth at a local damage area, if it were possible, would not lead to a direct interpretation of the overall material response.

Although fatigue lives may be long at given stress condition failure is defined as total separation, significant damage may be generated very early in the load history [4]. This can cause degradation (in the material properties) that renders the material incapable of meeting the originally specified structural requirements. In wind turbine applications, a loss of modulus above a particular value will allow the blade to have a much greater deflection than originally expected and may allow the blade to hit the tower. The question that is immediately raised in the wake of this seemingly complex information is this: is there a measurable parameter (or combination of several parameters) that can be effectively used to quantify the damage present in these materials? Furthermore, can that parameter (or parameters) be incorporated in a failure criterion to predict when the material can no longer fulfill its design objective? There is increasing evidence that the reduction in the stiffness of the material may be such a parameter, in some situations.

Stiffness change is directly related to damage and therefore is an appropriate design parameter and failure criterion for many components which incorporate composite materials. For example, cracking develops in the off-axis plies during cyclic loading so that cracks open during tensile loading; thus, the apparent average material modulus is reduced under tensile loads [4]. Unlike strength, which may actually increase in certain practical design situations,

stiffness decreases monotonically as damage increases. More importantly, the change in stiffness of a component due to damage can be measured nondestructively in real time while strength measurements must be made by destructive methods. Stiffness can also be measured by applying a remote or local loading and measuring relative local elastic constants using strain gages, or global moduli over a large gage section using extensometers or other deflection transducers. In addition, certain elastic constants may be measured ultrasonically using longitudinal and shear wave transducers [4].

Literature Review

Fatigue Damage Development The fatigue damage and failure of polymer matrix composites have been studied extensively, although many of the investigations into unidirectional ply fiberglass fatigue were limited to about one million cycles. Charewicz and Daniel [2] presented a study of monitoring fatigue damage in cross-ply graphite/epoxy composites by nondestructive testing techniques (X-ray). It was experimentally shown that five different damage mechanisms were observed: transverse matrix cracking, dispersed longitudinal cracking at low stress (long fatigue life), major localized longitudinal cracking at high stress (short fatigue life), delaminations along transverse cracks and local delaminations at the intersections of longitudinal and transverse cracks. Failure patterns vary with stress level

and number of cycles to failure. Under monotonic loading failure is brittle-like and concentrated. At high stresses and short fatigue lives failure results from few localized flaws, whereas at lower stresses and longer fatigue lives failure results from more dispersed flaws. Variations of residual modulus were measured as a function of cyclic stress level and number of cycles. The residual modulus showed a sharp reduction initially, followed by a more gradual decease up to failure. A cumulative damage model was proposed based on residual strength and the concept of equal damage curves.

Studies by Reifsnider and coworkers led to the clearest definition of typical fatigue damage in multidirectional laminates [5,6]. Masters and Reifsnider [5] performed an investigation of unidirectional ply graphite/epoxy laminates and described the failure mechanisms. Two quasi-isotropic configurations were studied: $[0/\pm45/90]_s$ and $[0/90/\pm45]_s$. The specimen geometry is illustrated in Figure 1. The cumulative damage data developed in their study indicated that the $[0/\pm45/90]_s$ and $[0/90/\pm45]_s$ graphite/epoxy laminates developed two distinctly different crack patterns (see Figure 2). That is, the saturation spacing values for the two laminates $[0/\pm45/90]_s$ and $[0/90/\pm45]_s$ are distinctly different. These patterns were created by the formation of transverse cracks with a regular spacing (a saturation spacing) in each off-axis lamina. Testing data revealed that this spacing was unique for each lamina in the laminate.

Reifsnider *et al* [6] reported extensive research with unidirectional ply carbon fiber/epoxy laminates with 0°, 90° and ±45° plies at low and moderate cyclic stresses. Initially, cracks occurred parallel to the fibers in the matrix of the off-axis plies either in the matrix material, or more commonly in the interface between fiber and matrix. This is commonly called either matrix cracking or interfacial debonding. These initial cracks formed and met axial plies and eventually began to cause damage in these main load bearing plies. This damage came in the form of broken fibers and delamination. At some point, the amount of damage in the laminate tended to level off for a period of cycles because the stress level between cracks was not sufficient to cause further cracking. This state is called the Characteristic Damage State (CDS). Further cycling beyond this point would cause delamination and fiber failure in the axial plies, eventually generating total separation [6]. Reifsnider has suggested the existence of a characteristic damage state for polymer matrix composites which forms independently of load history and is determined only by the laminate properties, their orientation and their stacking sequence. Sun and Jen [7] have similarly investigated matrix cracks and their effect on ultimate laminate strength in $[0/90/45]_s$ type graphite/epoxy laminates.

The effect of ply thickness on fatigue and static damage growth of matrix cracks in crossplied carbon/epoxy laminates

was studied by Lafarie-Frenot and Henaff-Gardin [8]. In their studies, tension-tension fatigue tests were conducted on two equivalent lay-ups, whose only difference consists in the stacking sequence and in the resulting 90° ply thickness. The 90° ply thickness was shown to have a considerable influence on the crack distribution in the transverse ply and on the fatigue crack growth rates. Herakovich [9] concluded that the thinner 90° ply would induce a longer crack onset delay, lower crack growth rates and smaller cracked surface areas, even though they would lead to higher edge crack density.

Dharan [10] investigated the failure mechanisms of unidirectional $[0°]_n$ composites. Specimens were made by filament winding the glass fiber roving and vacuum impregnating with a low viscosity room temperature curing resin. The fatigue response could be divided into three distinct life ranges. In the first region, there was a small dependence of the fatigue life on cycling. Behavior was believed to be dependent upon the fiber mean strength and strength distribution. In the second region, the logarithm of the maximum applied stress decreased almost linearly with the logarithm of the number of cycles to failure. Fatigue failure in this region was reported to occur by the growth of matrix microcracks, which lead to preferential fiber failure, and was followed by interfacial shear failure. In the third region, the applied stress was below the microcrack initiation stress and none of the few specimens tested failed. Unlike behavior

in the first two regions, where defects were formed in the first cycle and subsequently propagated, most of the cycles in this stage were used in crack initiation. These observations are contrary to those of Mandell [11] and coworkers, who found that the fatigue of unidirectional $[0°]_n$ composites with glass and carbon fibers respectively, is due to fiber failure, and is independent of matrix cracking.

Fatigue Lifetime The most widely accepted relationships (S-N curve) which correlate the maximum cyclic stress level to the fatigue life of uniaxially reinforced polymer composites take the form [12]

$$S/S_o = 1 - b\log(N) \qquad (2.3)$$

$$S/S_o = N^{(-1/m)} \qquad (2.4)$$

where S is the applied maximum stress, S_o is the single cycle (static) strength, N is the number of cycles to failure and b and m are material constants. Equation (2.3) yields a linear S-N curve on a plot of S *vs.* log N while Equation (2.4) is linear on a log-log plot. Equation (2.4) derives from integration of the Paris fatigue crack growth law

$$da/dN = A(K_{max})^m \qquad (2.5)$$

where a is the crack length, K_{max} is the maximum stress intensity factor (ΔK is more commonly used) and A is a constant; m should be the same as in Equation (2.4). Typical

m values for thermoset materials lie in the range of 11 to 14 [12]. This observed behavior trend correlates with fatigue crack growth predictions generated using fracture mechanics.

Mandell *et al.* [1, 13] recently investigated the high cycle fatigue behavior of wind turbine blade materials. Coupon testing was carried out under constant amplitude fatigue loading to beyond 10^7 cycles for most materials. The unidirectional materials performed close to expectations despite fiber misalignment; a power law trend appeared to provide the best fit to most of the data. This may imply that the lifetime was dominated by the matrix cracking along misoriented material, as the power law exponent correlates with the exponent obtained in ply delamination tests. Materials with triaxial (0°/±45°) reinforcement showed greater fatigue sensitivity than expected, but lifetime trends flattened at high cycles. Failure of the triaxial material appears to be dominated by cracking in the ±45° plies, which was not anticipated. While it was expected that these plies would fail first resulting in matrix cracks, this was not expected to lead to failure of the 0° strands. Effects of specimen width were studied by a comparison of data for 1.0 and 2.0 inch wide specimens. The study reported similar lifetimes at similar stress levels for the different width coupons. However, it is difficult to associate particular fracture modes with the trend of the data [13, 14]. Many investigations were also conducted to determine the *S-N* type

fatigue response to various fiber/matrix combinations, fiber strand size and volume fractions.

Residual Properties - Strength Determinations of residual (remaining) strength at different stages of fatigue lifetime were performed by several researchers. Charewicz and Daniel [2] investigated residual strength at different stages of fatigue lifetime for cross-ply graphite/epoxy laminates. It was shown that the fatigue sensitivity deceased with the number of contiguous 90° plies. The strength of a glass fiber reinforced composite decreased with increasing cycles, although there was much associated scatter. The residual strength showed some characteristic features: a sharp decrease initially, then a near plateau in the middle part of the fatigue life, and a rapid decease in the last part of the fatigue life.

Residual Properties - Stiffness The above *S-N* fatigue investigations gave insight into many of the fatigue damage mechanisms as noted. However, these *S-N* data only indicate the number of cycles that a specimen can withstand at a prescribed stress, and do not indicate how much damage the composite experiences before fracture. If the composite accumulates internal fatigue damage which reduces the laminate stiffness significantly, the composite may no longer meet the structural requirement although it still can carry the

required load. Investigators have realized the need for an alternative measure of fatigue damage instead of specimen fracture.

Reifsnider, Stinchcomb and O'Brien [15] have suggested the use of stiffness reduction as a damage parameter and criterion for fatigue failure in polymer matrix composites. In their studies, it was shown that the percent change in longitudinal static stiffness of a boron/epoxy laminate correlated both quantitatively and in lifetime trend with the amount of debonding and matrix crazing generated in the laminate during fatigue loading. Compliance (reciprocal of stiffness) and totalized acoustic emission from damage events were observed to increase [16] during fatigue tests.

By using stiffness reduction as a damage parameter, Daniel and Lee [17] have studied damage development in five cross-ply graphite/epoxy laminates under monotonic loadings. The laminates exhibited three characteristic ranges of varying stiffness. The first range was linear elastic and was characterized by the absence of any measurable damage. The second range was one of decreasing stiffness and corresponds to damage initiation and growth in the form of transverse matrix cracks in the 90° plies. These cracks increased in density up to the limiting value defined by the characteristic damage state discussed earlier. The third range in the stress-strain behavior was a nearly linear one of stabilized or even slightly increasing stiffness following the CDS and

reflected the stiffening behavior of the undamaged 0° plies. The predominant form of damage in all laminates was transverse matrix cracking monitored by X-radiography.

Hahn and Kim [18] suggested using the changes in the secant modulus as a measure of the damage extent in polymer matrix composite materials which have been subjected to fatigue loading. A plot of compliance versus total acoustic emission showed a very definite relationship between the time resolved stiffness of the specimen and the damage which develops during fatigue. However, there has been no comprehensive investigation to date on fiberglass/polymer matrix composites utilizing stiffness or a similar mechanical response to evaluate the fatigue damage process during high cyclic loading. Further research needs to be conducted to describe the fatigue damage mechanisms that might be responsible for the laminate degradation as reflected by reduced stiffness; is it 0°fiber fracture, matrix cracking, delamination or combinations of several events that are primarily responsible?

Nondestructive Evaluation Significant advances have been made in the area of non-destructive evaluation (NDE) techniques such as optical microscopy, X-ray and C-scan ultrasonic techniques applied to polymer matrix laminates for assessing their initial quality and accumulated damage. Davis [19] and Knott and Stinchcomb [20] discuss some of the

advances and problems concerning the non-destructive inspection of composite materials. The edge replication technique was first used to monitor damage in composite material by Stalnaker and Stinchcomb [21]. With this procedure of replicating edge cracking with plastic tape it is possible to obtain rapid, highly detailed permanent records of the entire specimen edge at different stages of lifetime.

Fatigue Failure Criterion Extensive research has been performed to characterize the residual strength degradation in order to predict the fatigue life of composite laminates under cyclic loading [22,23,24]. The fatigue life prediction of graphite/epoxy cross-ply composite laminates was carried out by Lee et al. [25]. The predicted fatigue life consists of two parts. The first part corresponds to the first stage of damage development consisting of transverse matrix cracking and crack multiplication up to the limiting characteristic damage state (CDS). This stage is based entirely on the state of stress in the 90° layer as it is being damaged and on the *S-N* curve of the 90° lamina. The second part of the fatigue life following attainment of CDS is based on the state of stress in the 0° plies and the *S-N* curve of the 0° lamina. It is assumed that the 0° plies within the damaged laminate behave under cyclic loading like a 0° unidirectional laminate. The total life predicted is taken as the sum of the two parts. Predicted results were in good agreement with experimental

results. However, the fatigue damage mechanisms in a cross-ply laminate are very different from those in a triaxial laminate with a stranded structure of ±45° and 0° material. More efforts need to be made on predicting fatigue life for more complicated triaxial (0/±45) laminates.

Another approach for predicting the fatigue life of composite laminates is by use of the residual stiffness degradation characteristics. Hahn [18] and Hwang [26,27] have suggested and developed a secant modulus criterion and a failure strain criterion respectively that would allow laminate fatigue failure to be predicted while tests were underway. Fatigue failure could be anticipated simply by monitoring static stiffness or strain at various intervals in the fatigue life and comparing measured changes to the secant modulus loss measured in a static tensile strength test on identical laminates. The secant modulus criterion may be stated as follows. When the static secant modulus, E_f, measured during fatigue, degrades from its initial tangent modulus, E_o, to the secant modulus, E_s, measured in a static ultimate strength test, regardless of load history, fatigue failure occurs. A corresponding strain to failure criterion is "failure occurs when the fatigue resultant strain reaches the static ultimate strain". Furthermore, glass fiber laminates, with a higher fiber strain capability, have been found to fail at accumulative strains below half of the static monotonic strain to failure [12].

Hahn and Kim [18] have also suggested that the change in the secant modulus can be used as a measure of damage extent in fatigue tests. To monitor the change in fatigue secant modulus, they would statically load the specimen to the maximum cyclic stress level and record the value of the secant modulus for laminates after a certain number of cycles.

O'Brien et al. [28] have tested the secant modulus criterion. Real-time fatigue failure was predicted using this secant modulus criterion for load-controlled, constant amplitude, tension-tension cyclic loading of $[0/\pm45/90]_s$ boron/epoxy composite laminates. The secant modulus criterion successfully predicted fatigue failure in $[0/90/\pm45]_s$ boron/epoxy laminates subjected to blocks of increasingly severe, constant-amplitude cyclic loads. However, it could not successfully predict fatigue failure in $[0/90]_s$ boron/epoxy laminates under similar loading conditions. Hence, they concluded that the modulus loss during the fatigue testing is load history dependent. The applicability of the secant modulus criterion for different materials, loading conditions, and stacking sequences is questionable.

In an effort to establish a valid fatigue failure criterion, a cumulative secant modulus criterion was investigated in the present study. This criterion has been first used as the basis of a mathematical model for predicting fatigue life by Hwang and Han [29]. This criterion states that the laminate would fail when the cumulative secant

that the laminate would fail when the cumulative secant modulus measured during fatigue was reduced to within the range of static secant modulus.

Delamination

Introduction

Delamination is one of the critical issues in the evaluation of durability and damage tolerance of laminated composite structures [30]. The problem of delamination between plies has been extensively studied in the context of free edges of test specimens such as Figure 3.

The principal reason for the existence of interlaminar stresses is the mismatch of Poisson's ratios ν_{xy} and coefficients of mutual influence m_x and m_y between adjacent laminas. If the laminas were not bonded and could deform freely, an axial loading in the x direction would create dissimilar transverse strains ϵ_{yy} in various laminas because of the difference in their Poisson's ratios. However, in perfect bonding, transverse strains must be identical throughout the laminate. The constraint against free transverse deformations produces normal stress σ_{yy} in each lamina and interlaminar shear stress τ_{yz} at the lamina interfaces. Similarly, the difference in the coefficients of mutual influence m_x and m_y would create the interlaminar normal stress σ_{zz}. However, the glassfiber reinforced laminate has

a lower mismatch of Poison's ratios and coefficients of mutual influence than the carbon fiber reinforced laminate does. The existence of delamination and delamination growth in a structure redistributes the stresses in the plies of the laminate, and may significantly influence the in-plane stiffness, strength and fatigue life of the structure. Delaminations may form and grow under both static and cyclic tensile loading. Delamination may develop during manufacture due to incomplete curing or the introduction of foreign particles, may be induced by in-service events such as impact or may result due to the presence of interlaminar stresses that develop at stress-free edges or discontinuities from the mismatch in elastic constants of the individual plies. These edge delaminations typically occur between 90° plies and adjacent angle plies, with delaminations forming initially in a thumbnail shape, and rapidly becoming a delaminated strip that grows across the specimen width [31]. Another source of delamination is matrix ply cracks running parallel to the fibers in a ply. The interlaminar normal stress, σ_z, that develops in the ply interface at matrix crack tips may cause local delaminations to form and grow [32].

Pipes and Pagano [33] concluded that edge delaminations are caused by the interlaminar normal stresses σ_z that peak at the free edge. The laminate geometry and stress direction are described in the Figure 3. In this figure, *x* axis represents the loading direction, and *x* and *y* axes are in the plane of

the laminate, and the z axis is normal to this plane. The stress components σ_x, σ_y, τ_{xy} are called in-plane (intralaminar) stresses, whereas σ_z, τ_{xz}, τ_{yz} are called interlaminar stresses, with a z component out of the plane of the laminates. Pipes and Pagano speculated that a mathematical singularity exists because σ_z increases very rapidly near the free edge. Hence, the mere fact that a very high interlaminar normal stress σ_z exists leads to the conclusion that laminates should be changed to minimize the stresses.

Literature Review

In recent years, a large amount of attention has been given to delamination problems in laminated composites [34]. In the case of free-edge delamination, O'Brien [35] has shown that the predominant failure mode for laminate free edges is Mode I delamination, i.e., opening mode delamination due to high interlaminar normal stress. Herakovich [36] found that the edge delamination strength of a given laminate was dependent upon the mismatch of the Poisson's ratio and the mutual influence coefficient between the adjacent layers. It has also been found that reducing the Poisson's ratio mismatch between adjacent layers could significantly decrease both interlaminar normal and shearing stresses and subsequently increase the laminate strength. The effects of laminate width and loading conditions on the free-edge delamination were

studied by Murthy and Chamis [37]. They found that axial tension causes the smallest magnitude of interlaminar free edge stress compared to other loading conditions; laminates with practical dimensions may not delaminate because of free edge stresses alone since the magnitude of these stresses are found to be quite insignificant.

Although delamination may not immediately cause catastrophic failure of the structure, it often hastens component repair or replacement, which results in increased life costs [38]. Therefore, designers have had an increasing concern to find ways to delay or prevent delamination in structural design. Research efforts have been directed towards suppressing or arresting this failure mode and understanding the failure mechanism behind it.

These efforts have led to the improved development of delamination resistance, achieved by both improving materials and tailoring the laminate in construction [39].

Initiation and growth of delamination is dependent upon interlaminar fracture toughness or the interlaminar stress field in the vicinity of the delamination front or both. Therefore, raising the fracture toughness or reducing the interlaminar stresses or both are key guidelines to developing the delamination resistance. These guidelines generally fall into one or both of two categories: improvement of materials or laminate construction.

The laminate construction approach often taken is to

reduce the magnitude of either interlaminar stresses or delamination initiation. This results in reduction of the strain energy release rate, the source of energy available for delamination growth. Consequently, delamination resistance can be improved. The following two innovative design methods for suppressing or arresting delamination have been developed.

Stitching: Various studies have shown that through-the-thickness stitching offers improved capability to withstand out-of-plane tensile loads as well as suppress or delay delamination growth. Stitching locks the plies together, inhibiting delamination from direct out-of-plane loading, such as impact [39]. For delamination at free edges as a result of in-plane loading, it was found by Mignery [40] that stitching could effectively arrest edge delamination but might have adverse effects on the strength and fatigue life of the fiber-dominated laminates. In their study, a two-dimensional finite element analysis is used to calculate interlaminar normal stress and strain energy release rate, which represents the energy per unit delamination area required to extend the delamination, for stitched and unstitched laminates. Their analysis results indicated that the introduction of stitching would cause little change in the interlaminar normal stress but reduce delamination crack opening. The strain energy release rate, which can be correlated with delamination crack growth rate, was reduced as a result of the delamination being "bridged" by the stitch.

Edge Cap and Wrapped edge Reinforcement: Reinforcement of the free edge can be achieved by wrapping the edges of the laminate with composite or metal caps. There has been some work done with this technique in recent years. Kim [41] used a fiberglass cloth and Howard et al. [42] used a Kevlar layer hybridized with graphite/epoxy layers to cap the edges of a graphite/epoxy laminate. The results from this technique indicated that static and fatigue strength were increased if the edges were capped. The improvement of laminate strength in the capped laminate was attributed to the reduction of the interlaminar normal stress and not the shear stress. However, capping the edges may increase the manufacturing cost and may also increase the bending rigidity. The capped laminates were fabricated with the continuous fibers at the edge. Another approach, folding or wrapping the plies at the free edge, was studied under static loading conditions by Tan [43]. In his research, the folding technique was applied to make $[\pm\theta^\circ/\mp\theta^\circ]_s$ graphite/epoxy family of laminates. The modulus and strength of the folded laminates were characterized and compared to the conventional laminates made by cutting the edge to see edge effects on the static tensile behavior of the angle ply laminates. Both static tension and compression tests showed that the folded laminates were significantly stiffer and stronger than conventional laminates. This is simply because the wrapped laminates have no free-edges. The folded edges were like constraints to the free-edges of the laminates.

Introduction to This Study

Much of the foregoing research on damage development was done in the area of carbon reinforced polymers under fatigue loading; glassfiber reinforced polymers under fatigue loading were only tested to low or moderate numbers of cycle range. There is a clear need for fatigue data in the high cycles (*e.g.* beyond one million cycles). There have been many attempts to analyze complex damage states, but much more effort will be required before these studies yield readily applicable results. The characteristics of damage states in each new type of composite structure require investigation, as do potential failure criteria.

The main objective of this investigation was to address these issues for stranded triaxial reinforced glass/polyester laminates used for many applications. The development of methods for accurately documenting damage development in composite materials by monitoring change in the stiffness and crack density have been pursued as well as the characterization of damage initiation, growth, and failure modes. Several series of fatigue tests were conducted on glass/polyester $[0°/\pm45°]_4$ laminates. Plots of the stiffness response in the loading direction were recorded at intervals during the cyclic life and used for assessing the changes in laminate properties. The tested specimens were then examined microscopically to identify the extent of cyclic damage.

These results were used to correlate laminate stiffness and matrix crack density.

For fatigue life prediction, Hahn and Kim [18] suggested and developed secant modulus criteria (see Figure 4). However, it was found by O'Brien *et al.* that this criterion is load history dependent. A generally accepted fatigue failure criterion for composite materials has not yet been defined. In my current study, the secant modulus criterion was tested and a modified fatigue modulus criterion was proposed to predict the fatigue failure for triaxially reinforced laminates. Figure 5 shows the hystersis loop diagrams for triaxial laminates to determine the static and fatigue secant moduli. Because the failure modulus criterion assumes that secant modulus loss is independent of load history, a series of tension-tension fatigue tests at different stress levels were conducted to estimate the residual secant modulus loss prior to failure.

The sensitivity of fatigue results to the cut-edge geometry used for coupon as in Figure 1 is a significant uncertainty; does the machined edge lead to edge delamination induced failures? An objective of this study was to subject standard machined edge and wrapped edge laminates to fatigue loading to failure and thus examine influence of free coupon edge on failure. It was expected that the folded laminates which had continuous fibers at the edge would have better fatigue behavior than those without a folded edge if

delamination crack initiation or delamination growth at the edge was the dominant failure mode.

Two material systems (Materials V and W) were tested under the fatigue loading conditions to study the effects of variations in triaxial reinforcement on the fatigue behavior. These two material systems were made using different stitching patterns. The effects of the different stitching patterns on the fatigue resistance was evaluated by comparing corresponding *S-N* curves. Additionally, damage initiation, growth and failure mode were then characterized using optical microscopy and by recording stiffness reductions during fatigue. The observations that were made should aid in the understanding of changes in laminate response during fatigue testing, such as fatigue resistance, stiffness reduction, damage initiation, damage growth, and failure modes for the laminates which were made with different stitching patterns.

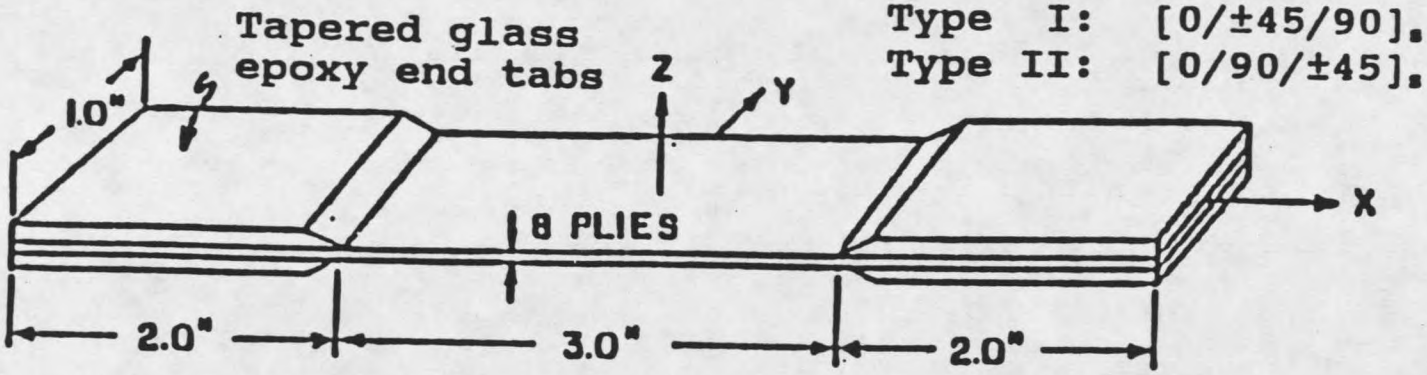

Figure 1. Specimen configuration [5].

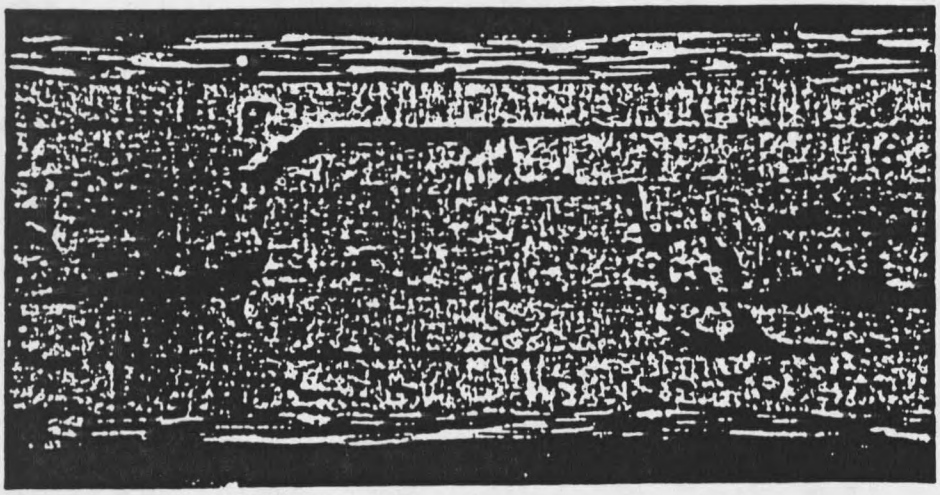

(a)

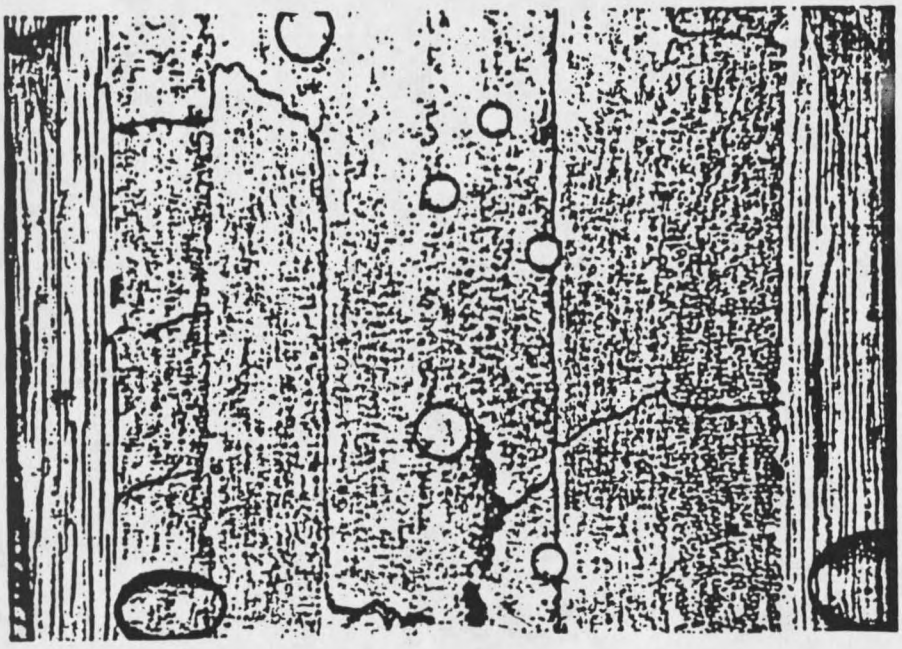

(b)

Figure 2. Damage features in (a) $[0/\pm45/90]_s$ and (b) $[0/90/\pm45]_s$ laminate [5].

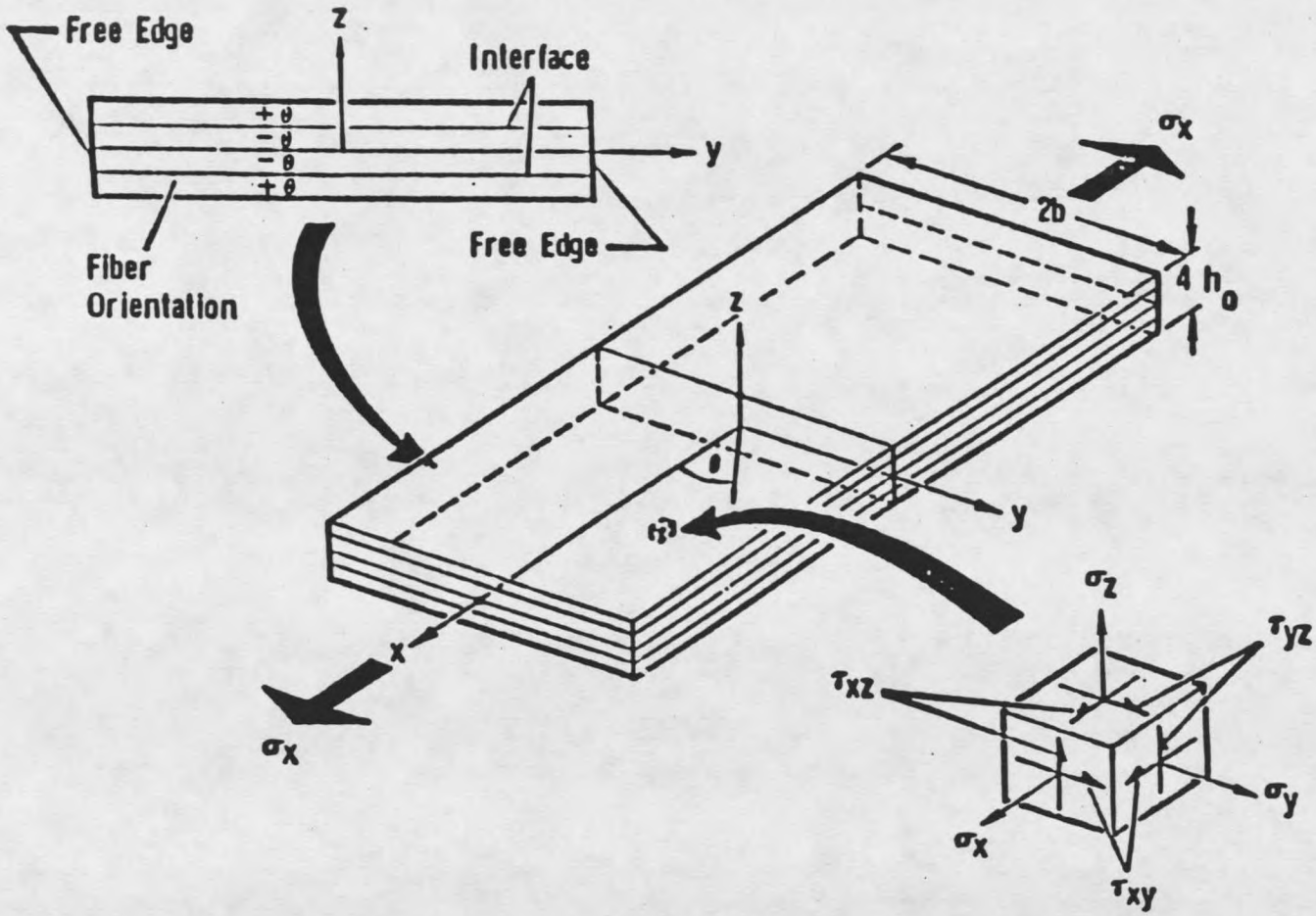

Figure 3 Laminate geometry and stress direction [30].

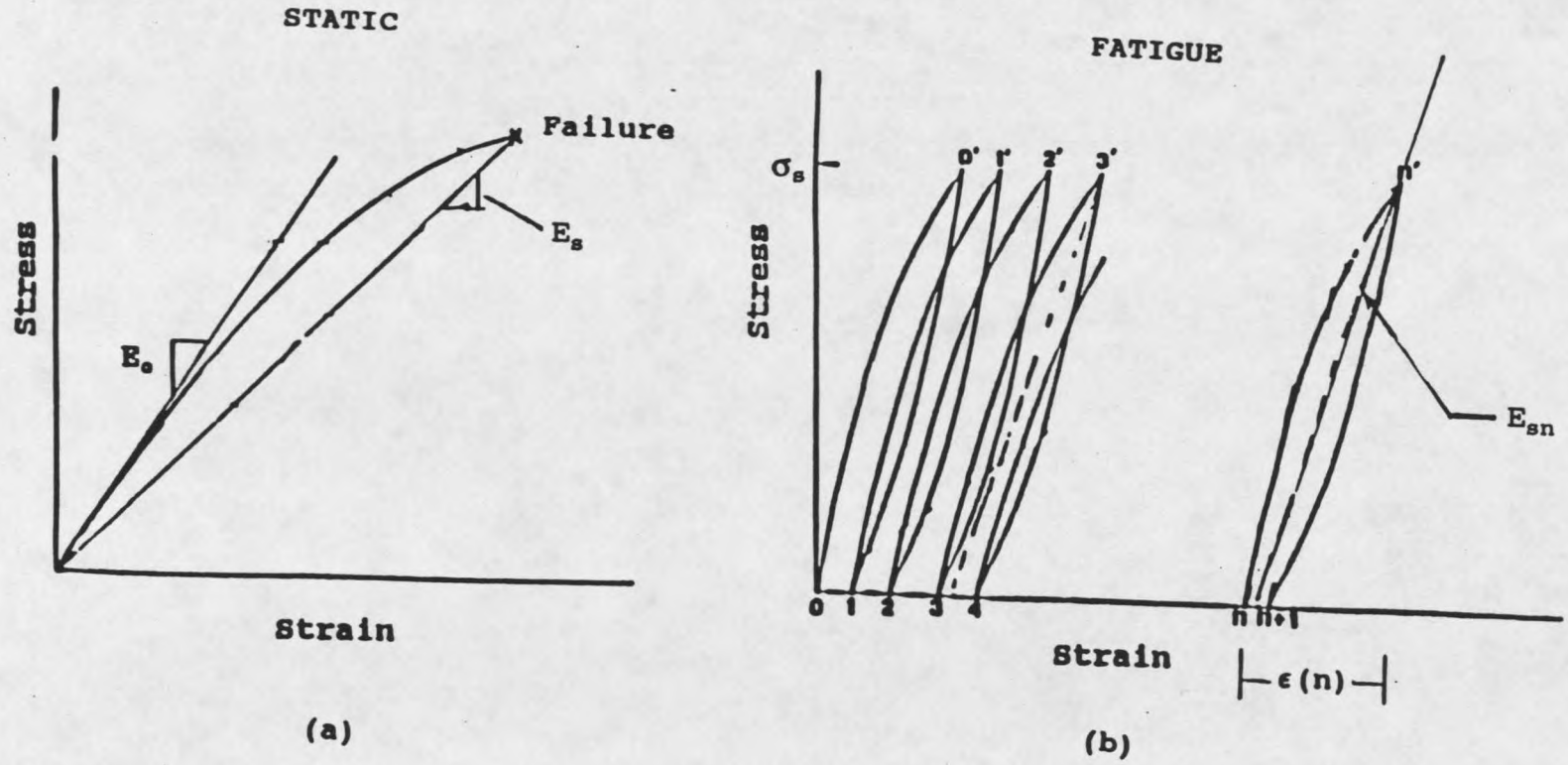

Figure 4. Fatigue secant modulus criterion [18]: failure when $E_{sn} = E_s$.

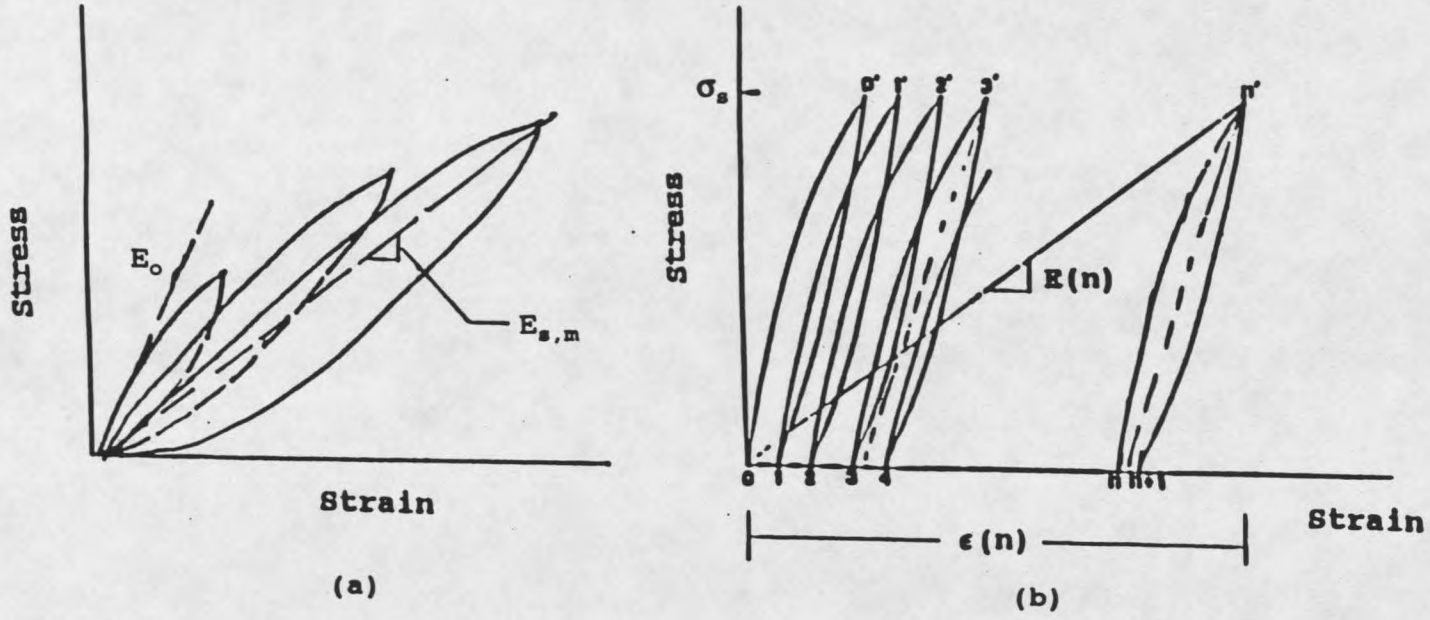

Figure 5. Schematic of cumulative secant modulus criterion [29]: failure when $E(n) = E_{s,m}$

CHAPTER THREE

EXPERIMENTAL TESTING PROGRAM

The objective of the experimental testing program was to accumulate static strength, dynamic fatigue and damage development data for triaxially reinforced fiberglass composite materials.

An attempt was made to eliminate as many variables as possible from one set of laminate data to another. Therefore, all of the static and fatigue data were obtained utilizing the same test equipment and environment. Also, all of the composite specimens had nominally the same width and were obtained from the same manufacturer.

Testing materials, facilities and various methods of measuring static and fatigue properties are described in this chapter.

Tension and Tension Fatigue Testing

Materials

The materials used in this study were unidirectional ply glass fiber/polyester matrix composites comprised of 4 layers

of $[0°/\pm45°]_4$ defined in Table 1. Each layer is composed of tightly wrapped strands, with the three layers also stitched together. Stitching was by an organic fiber yarn. Each laminate contained 6 plies (2 layers of triax, with three plies in each layer) on each side of the composite mid-thickness. The specimen layup and laminate definition are illustrated in Figure 6. Materials were supplied by Phonex Industries in the form of cured composites sheets.

All samples were post cured for 24 hours at 140°F. The reinforcement fabric used in these materials was supplied by Hexcel Corporation.

Materials V and W were conventional panels which were four layers thick. Their fatigue behavior was directly compared with that of the folded specimens of the same material (Material T and U). These folded edge triaxial samples were four layers thick formed in cross section by a double back "S" shape (see Figure 7).

Materials T and U were made in different stitching patterns. All stitching in Material T was at 0° or 45° directions, while stitching in Material U was in the 90° direction. Materials T, U, V and W were designed to examine the edge effects on fatigue properties of the triaxial laminates. Materials V and W were developed to investigate damage development and to examine the effects of different stitching patterns on the fatigue behavior of the triaxial laminate composites. Material V was stitched much more

tightly, as described later.

Specimen Preparation

Standard composite specimens were cut from cured composite sheets obtained from Phoenix Industries. The general test coupon geometry was an 8 inch long, 2 inch wide, flat specimen with a uniform, symmetric cross section (see Figure 8). Tabs were of rectangular shape approximately 2.0 inch wide and 2.0 inch long, with a 15° taper. The composite specimens were also abraded and solvent cleaned in the tab attachment regions. The tab face, which was to be attached to the ends of flat test coupons, was abraded using silicon carbide abrasive paper. The tabs were then adhesively bonded to the ends of the specimens with Hysol 9309.2 NA high toughness epoxy. The adhesive cure took place in one to two hours at room temperature, but specimens were allowed to cure for at least a day before testing. The special tab material in this area reduces stress concentrations, thereby promoting tensile static and tension-tension fatigue failure in the gage section. The guidelines for the standard geometry are defined by the ASTM D 3039-76, "standard test method for tensile properties of fiberglass-resin composites", and followed modifications described in Reference 44.

Equipment and Testing Procedure

The machines used for this research were a Material Testing System (MTS) 880 machine with a load capacity of 55000 pounds force (edge effect tests), and for the rest of the tests an Instron 8501 machine with a load capacity of 22000 pounds force, a hydraulic supply of 20 gallons per minute, a ten gallon per minute servovalve, a system pressure of 3000 psi and modular hydraulic grips. All tensile tests and damage development studies were performed with these setups. Figure 9 is a photograph of the Instron 8500. The Instron machine was controlled by an Instron Model 9500 controller and Instron computer software SR9 and FLPS.

Before testing, test sections of each specimen were individually measured for width and thickness with a micrometer to determine the cross-sectional area.

For the static strength test, the specimen was carefully mounted and aligned in the grips of the MTS or Instron machine. An extensometer unit was attached to the specimen to measure the global composite strain (change in length/original length) over a 1.0 inch gage section in the loading direction, while built-in force and displacement transducers measured applied load and overall piston deflection. The static specimens were loaded to failure with a speed of 1000 lb/min. The initial elastic modulus of the laminate was recorded from the stress-strain curve.

In a typical procedure used to evaluate the tensile fatigue behavior of a material, a specimen of the material was placed under a specific cyclic tension load condition for numerous cycles. Constant load (stress) amplitude-controlled tests were performed. The specimen was initially loaded to the mean cyclic stress level using a ramp wave generator at a speed of 1000 lb/min. The maximum cyclic stress amplitude was chosen for each laminate type to produce a desired lifetime range. A test was then run in load control with a constant sine wave input and constant stress ratio (maximum stress/minimum stress) R = 0.1, and the specimen was cycled between specified maximum and minimum loads so that a constant load amplitude was maintained (see Figure 10). In addition, the partially fatigued specimens were tested under tensile load to determine the residual Young's modulus in order to assess the cumulative damage during fatigue. The tension-tension fatigue cycling test procedure is described in ASTM D3479-76.

When the specimen failed during the fatigue cycling, a displacement limit was activated and the hydraulic pressure was cut off. The cyclic counter panel recorded the number of cycles to failure.

Experimental Data Reduction

All experimental data in this study were examined and reduced to yield several mechanical properties:

1. Initial elastic modulus
2. Ultimate static strength
3. Elastic modulus after n number of cycles
4. Number of cycles to fatigue failure, N

A detailed description of how each of the above mechanical properties were measured and their physical significance follows.

Initial elastic modulus The elastic modulus, E_o, is the modulus of the initial linear portion of the loading or unloading stress *vs.* strain curve. The initial elastic modulus is significant in that all later measurements of elastic moduli at n cycles will be compared to this initial modulus to give a measure of the reduction in stiffness during cycling at a particular stress level. The stiffness change will be correlated with the amount of internal fatigue damage suffered by the composite laminate. Therefore, any reduction in overall elastic modulus is taken to be due to cracks in the matrix or fiber /matrix interface, fracture of fibers, and/or delamination of the laminae.

Elastic modulus after n cycles The elastic unloading modulus was measured directly from the stress-strain curve at intervals throughout the life of the composite. The current modulus as a percentage of the initial elastic modulus at n cycles is given by

$$(E_n/E_o)\times 100 = \%E_o$$

This was plotted against the number of fatigue cycles, n, in order to present the modulus as a function of cycles at a prescribed stress ratio and maximum stress.

Number of cycles to fatigue failure The specimen lifetime, the number of cycles to total failure, N, was recorded by the counter panel within the closed loop testing system. The logarithm of lifetime, N, is plotted versus the maximum cyclic stress to establish the traditional S-N curve. This type of data indicates the lifetime for a particular maximum cyclic stress at a given stress ratio, R, and test frequency. The S-N curve does not, however, indicate the physical condition of the laminate at or before the established lifetime other than the fact that the laminate can maintain this stress condition to the defined lifetime, N, at which point it separated into two pieces.

Ultimate static strength The specimen was monotonically loaded at approximately 1000 lb_f/min until failure. The stress-strain response was recorded. The maximum stress at failure was determined from the stress-strain curve and was defined as the ultimate static tensile stress, UTS.

Damage Development Studies

In many composite laminates stiffness loss may reflect damage growth. Therefore, analysis and experiments were performed to correlate laminate stiffness and matrix crack density.

Constant amplitude, tension-tension, load controlled fatigue tests of $[0/\pm45]_4$ glass/polyester specimens were conducted at a frequency of 15 Hz. Laminate stiffness was measured during this initial loading. Then, the specimen was unloaded and matrix crack density was recorded using optical microscopy. Next, the specimen was reloaded to the mean stress and the stiffness of the cracked specimen was recorded. Next, constant-stress-amplitude cyclic loading was applied. The cyclic loading was interrupted at specified intervals to measure crack density at the free-edge of each specimen under a microscope, and a record of static stiffness as a function of load cycles was accumulated. Cyclic loading was terminated when the laminate failed. The relationship between stiffness and damage development was studied, and delamination and fiber fracture were also investigated.

The nondestructive and destructive techniques used for the examination and analysis of damage conditions produced by each of these test series were edge replication and microscopy of polished edges. The edge replicas of the various laminates were then examined and photographed using optical microscopy

to characterize the damage growth during the fatigue testing. The edge delamination was observed using X-radiography.

Specimen Preparation

Careful polishing of the edge of replication samples was necessary to clearly observe damage. First, grinding of the edges of the specimens was performed on a metallographic polishing wheel. Grinding (rough polishing) used successively finer abrasives of Struers silicon carbide polishing papers, from 1000 grit to 4000 grit. The specimen cross-section was microscopically examined between each step. Polishing used a slurry of 5-micron alumina power and water on a silk polishing cloth mounted on the polishing wheel, again examining the specimen regularly to monitor progress. Polishing was continued until virtually no scratches were visible on the surface of the specimen when observed with the microscope at a magnification of about 1000X, and the interfaces appeared continuous from fiber to matrix, so that subsequent damage growth was clearly visible.

Replication Process and Crack Measurement

Replication techniques have proven very useful in damage development studies of resin matrix composites [45]. The surface replicas are used to highlight transverse cracking and delamination, with specimen removal or destruction not

necessary.

During the fatigue loading, each test was interrupted periodically to obtain replicas at a progression of cycle levels. An imprint of the damage accumulation was obtained by applying cellulose acetate tape to the specimen edges. To make an edge replica, a piece of cellulose acetate was attached to the specimen edge using adhesive tape. The cellulose acetate was a thin film on the order of 3-10 mils thick. Next, a syringe was filled with acetone. The acetone was injected between the specimen edge and the cellulose acetate. After injecting the acetone, the cellulose acetate was pressed against the specimen edge. At least several minutes drying time was necessary before removing the replica from the specimen edge and attaching it on a microscope slide. Replicas, mounted on microscope slides, were then examined by optical microscopy.

The crack density was determined from the replicas. The number of cracks counted over a distance of about 2 inches was used to determine the crack density in number of cracks per inch of length along the specimen edge in the particular layer of interest.

Optical Microscope System

The microscope system consisted of an optical microscope, color video monitor, color TV camera, video measuring system, color video printer and translation stage as shown in Figure

11.

The camera (WV-CL110) was attached on the top of the optical microscope (Leitz Wetzlar, Model 563 486). The microscope was mounted on a vibration isolation platform (Kinetic Systems, Model 2212) to reduce the effects of floor vibration. A eyepiece of 10X and objectives of 2.5, 10, 50 and 100X were used to bring a maximum magnification of about 2000X.

The translation stage subassembly was below the microscope objectives. It consisted of an X-Y axis micrometer drive stage (Newport, Model M-481) for accurate movement of the specimen. The video monitor (Sony Trinitron, Model PVM-1342Q) with a measuring system (Boeckeler Instruments, VIA-100) was used for measuring the crack density and distribution. Photomicrographs of the samples were taken on a Kodak SV6500 Color Video Printer and a Kodak SV65 Color Video Finisher.

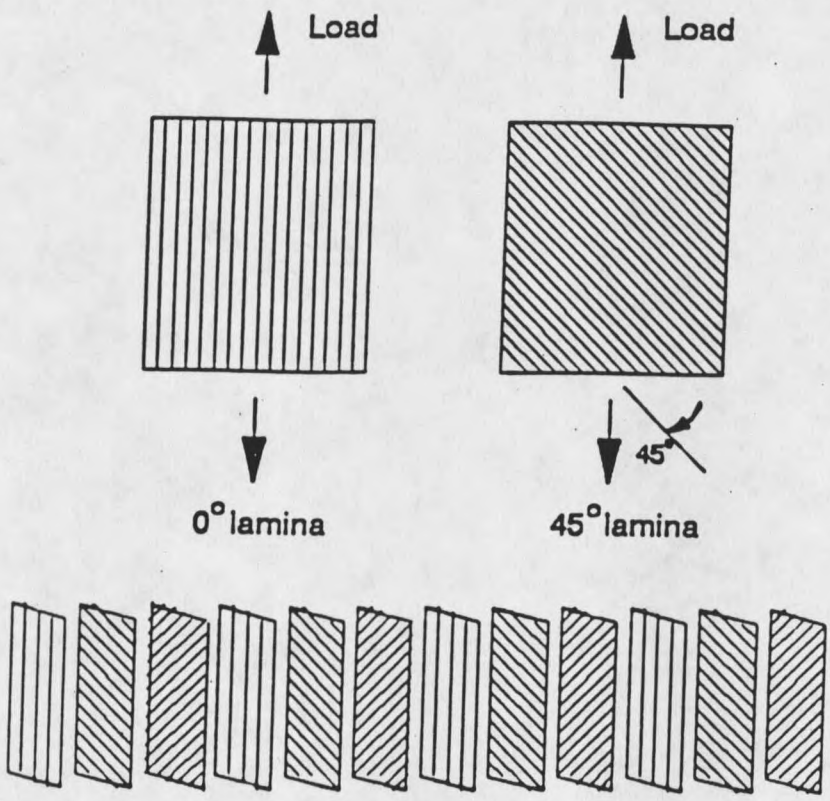

Figure 6. Lamina and laminate descriptions

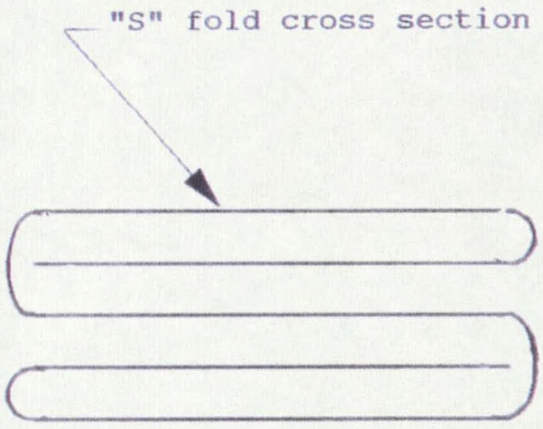

(a)

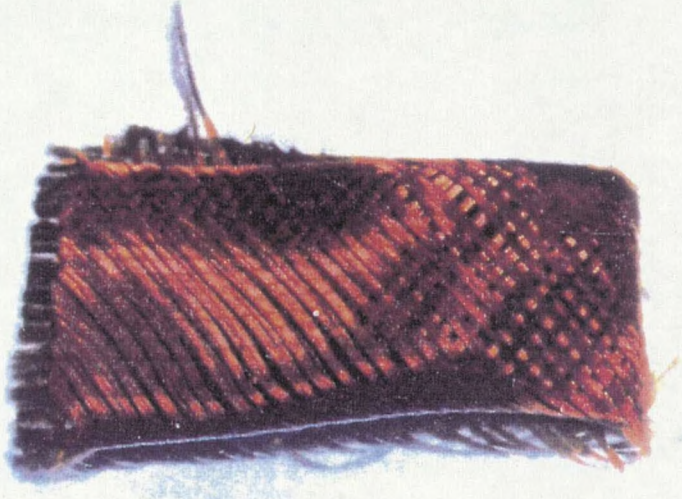

(b)

Figure 7. Wrapped laminate (Material W) geometry

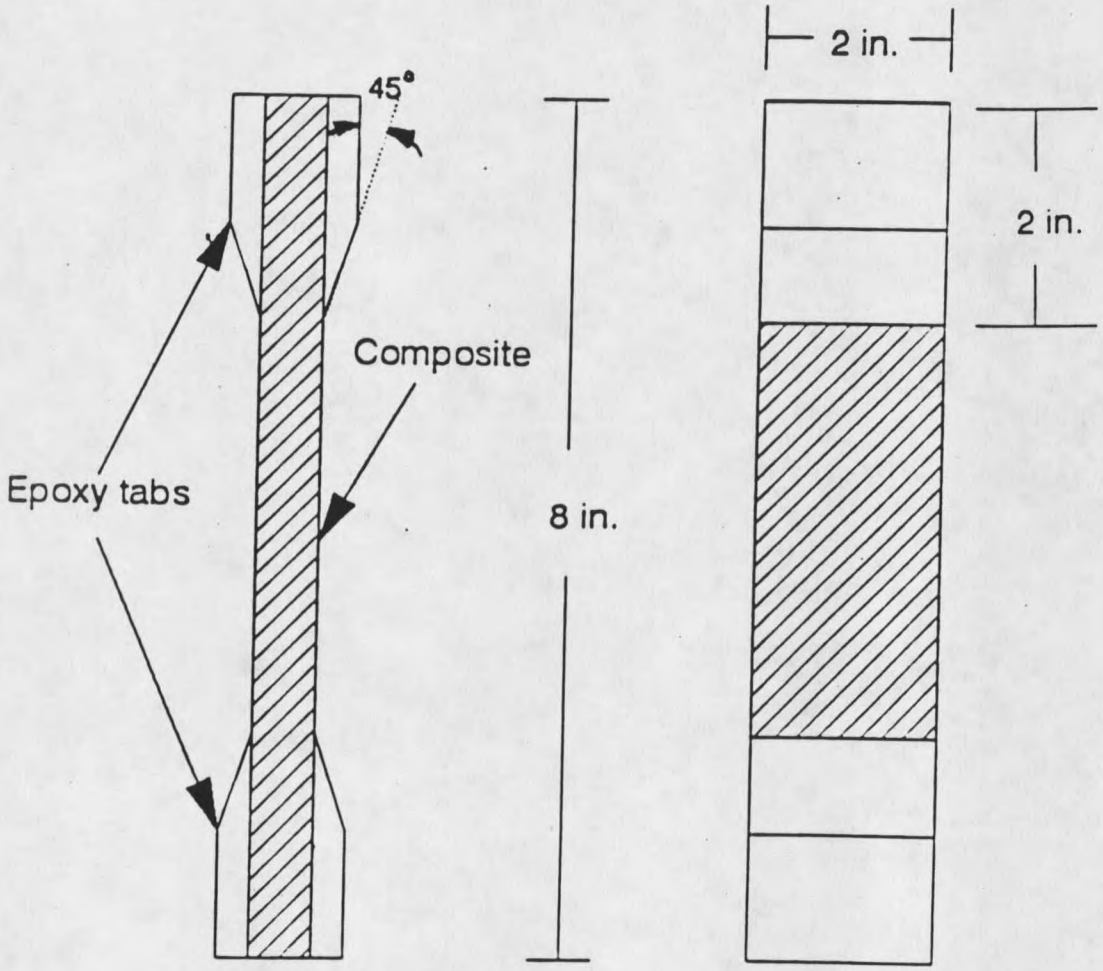

Figure 8. Tensile fatigue test coupon configuration.

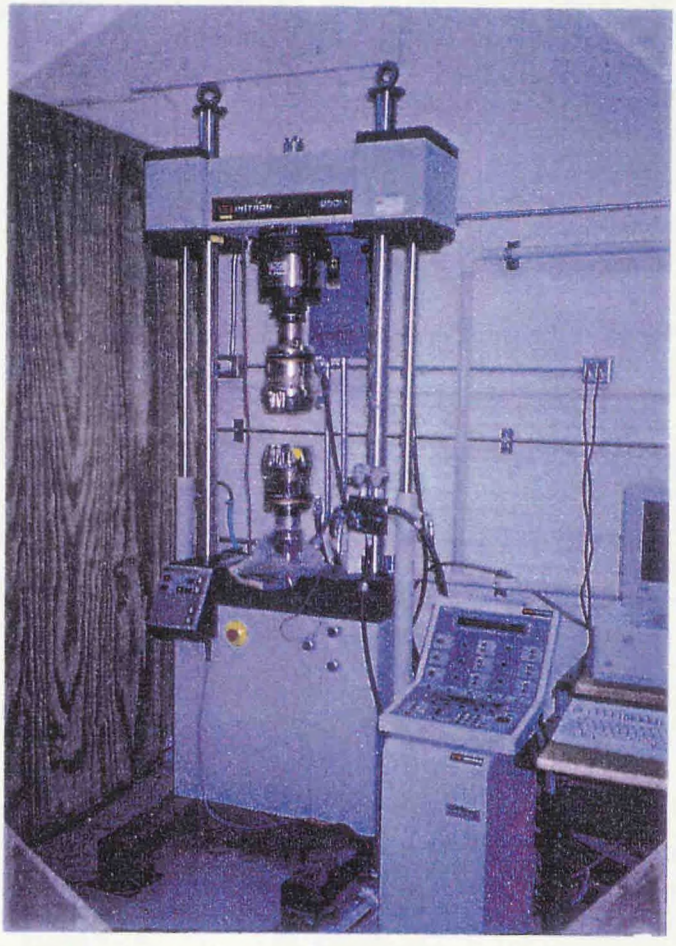

Figure 9. Photograph of Instron 8500 Testing System.

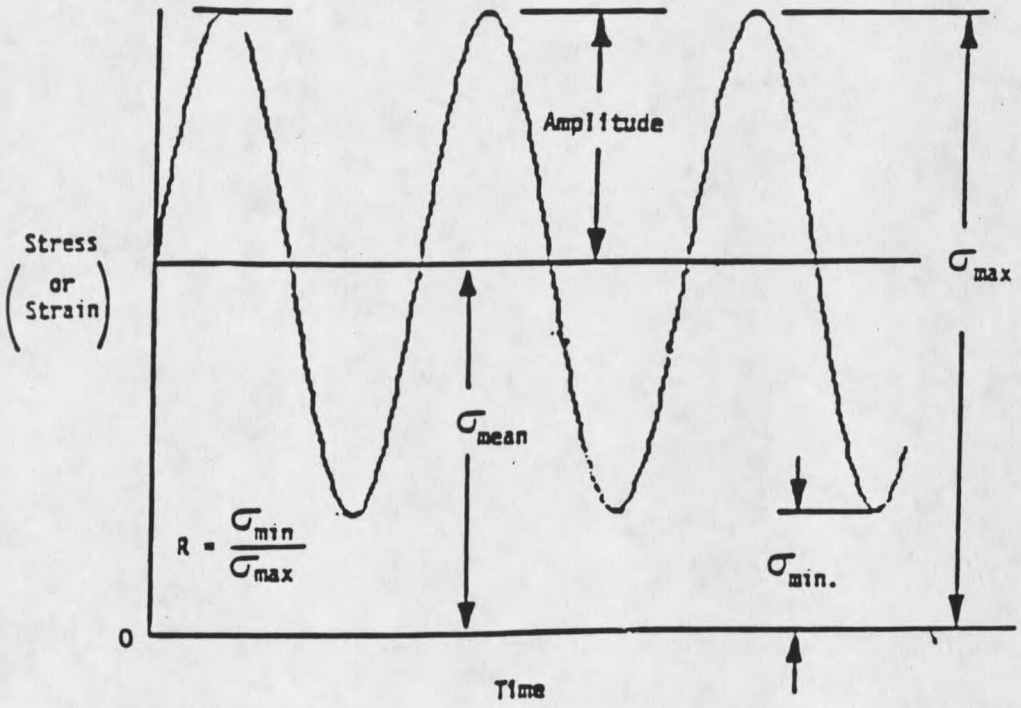

Figure 10. Stress-time diagram in a fatigue test[42].

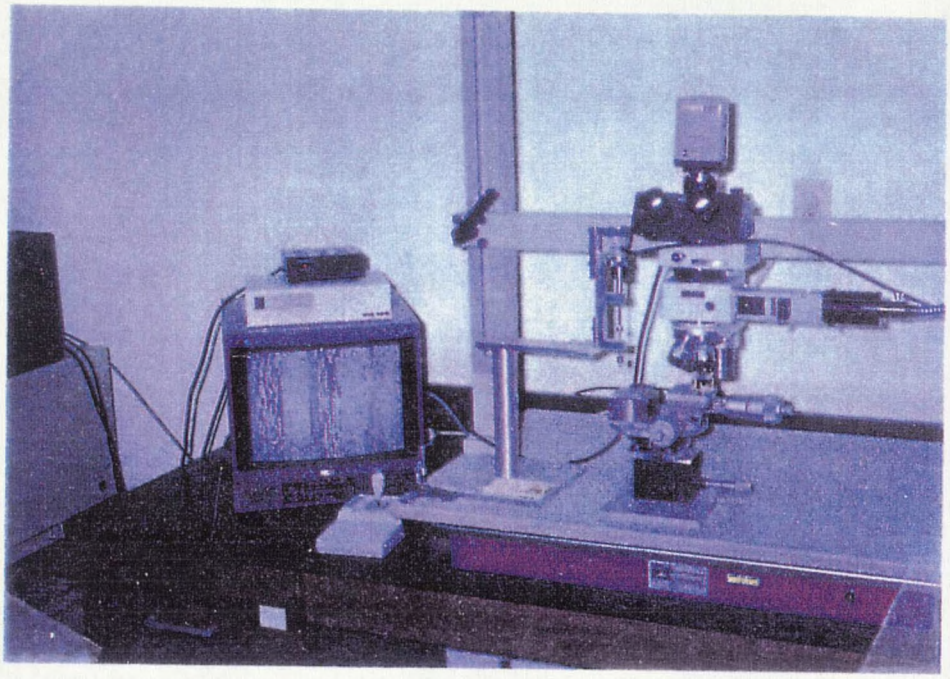

Figure 11. Microscope system.

CHAPTER FOUR

RESULTS AND DISCUSSION

The overall objective of this thesis was to develop an improved understanding of the long term fatigue behavior of triaxially reinforced glass-fiber/polyester matrix composites. Previous to this thesis, very little work had been reported on the mechanics of fatigue damage development in these materials under high cycle fatigue loading. In this study, the tension-tension fatigue behavior of $[0°/\pm45°]_4$ material was first studied to characterize damage development by monitoring the matrix cracking and changes in modulus with increasing cycles. The wrapped and unwrapped edge laminates were then characterized to observe any edge effects on the fatigue properties at various cyclic stress levels. Finally, to better understand the effects of the fabrication method on the fatigue properties, direct fatigue resistance studies were carried out on triaxial materials with different support stitching.

Fatigue Damage and Stiffness Changes

The standard specimens for Materials V and W (unwrapped edge) were prepared by standard machining methods (see Chapter 3) from a 12-ply $[0/\pm45]_4$ triaxial fiberglass reinforced composite plate. Material V had a 19 percent 0° fibers and 38 percent ±45° fibers. Material W had a 18 percent 0° fibers and 36 percent ±45° fibers. The ultimate tensile strength for Materials V and W were 54.3×10^3 psi and 49.5×10^3 psi, respectively. The static mode of failure for the triaxial materials was a brooming failure of the 0° and center ±45° fibers, with an associated debonding of some ±45° fibers (see Figure 12).

Several fatigue tests were conducted at two maximum stress levels, σ_{max} = 12500 and 15000 psi. The fatigue failures appeared to exhibit damage initiation, propagation and accumulation as described in Chapter 2. When plotted as total cumulative cracks per inch length along the specimen edge versus the number of cycles, a typical four-stage crack growth curve is observed for both materials. The shape of the crack growth curve in Figure 13 for short-life and long-life tests is similar and varies little from specimen to specimen. That is, from the early to late stages of specimen life, the varying relationship between cycle level and crack density show similar trends to that in Figure 13 for Material W at a maximum cyclic stress of 15000 psi. Each data point in this and following figures represents an average of three

measurements. The dashed line at the end of the curve indicates that high crack densities were evident at failure, but they could not be measured consistently. Stages (I), (II), (III) and (V) are marked on the figure. This partition of the crack density curve also serves to partition the dominant modes of fatigue damage that occurred in this laminate type, as will be shown in the following description of damage for each state of the $[0°/\pm45°]_4$ laminate type.

Stage (I) When the cycles were increased to a certain level, the laminate appeared to be undamaged, with no detectable cracks. Figure 14 shows an edge replica of a $[0°/\pm45°]_4$ specimen at the end of 1000 cycles with no detectable damage.

Stage (II) During this stage, initial matrix cracking in the ±45° plies started in the middle of the specimen gage length and the cracking spread rapidly along the edge toward the tab area with increasing cycles. The crack density-cycle curves are non-linear in this stage as shown in Figure 13. Stage (II) usually involved matrix cracking through the thickness of the off-axis (45°) plies and perpendicular (at least in transverse projection) to the dominant load axis (0° direction). Figure 15(a), (b) and Figure 16 show microphotographs and schematic view of transverse crack patterns as seen from the edge and surface of laminates at the end of the Stage (II). As shown in Figure 15(b), matrix cracking developed along the ±45° fibers. Notice that for

both of the applied cyclic stress levels, the matrix cracks were not uniformly distributed along the gage length as shown in Figure 15(b), which was contrary to findings for some triaxial or multidirectional laminates, from other investigators [46].

Figure 17 compares crack density in the ±45° plies of Material W for a static specimen as a function of applied stress level with the results for a fatigue specimen as a function of cycles at a constant maximum stress. During the fatigue testing, almost all of the observed modulus decrease is likely to be attributable to cracks in the matrix of the off-axis plies, since such cracks were the only observed damage of consequence. For the cyclic loading test, cracks developed quite early in the life and quickly stabilized to a very nearly constant density with a fixed spacing during Stage (II). However, the same behavior occurred for quasi-static loading, in the sense that crack development occurred over a small range of load and quickly stabilized into a pattern with the same spacing as for the fatigue crack pattern. This damage pattern is the so called characteristic damage state (CDS) for matrix cracking in laminates having off-axis plies. In fact, the two patterns, one fatigue testing and one static testing, were essentially identical regular crack arrays in a ply regardless of load history. Figure 18 shows that a saturation damage state existed for a given laminate geometry and load history no matter whether it

was tested under high or low cyclic stress conditions. These above results indicate that the CDS is independent of load history, consistent with Reference [44]. This Stage (III) of damage development began at approximately 60% of the lifetime of the specimen then the damage remained relatively unchanged for the remainder of the life for both cyclic stress levels as shown in Figure 17.

Having identified the damage development events in Stage (II), the consequences of those events are pursued. Figure 19 shows elastic modulus and crack density in ±45° plies in Material W as a function of loading cycles at a maximum cyclic stress of 15000 psi. The matrix cracks produced the expected reduction in the stiffness of the laminate. For triaxial laminates, the maximum laminate stiffness change was on the order of 15% at approximately 60% of its lifetime and then remained unchanged. Therefore, the change in fatigue elastic modulus could not be used to predict the fatigue lifetime. These changes in stiffness are generally not of great engineering concern except in areas where dynamic resonances may be important. Other damage at this stage was relatively minor. Some small delaminations confined to a boundary layer along the edge were observed. These delaminations actually appeared to mark the beginning of Stage (III) damage.

Stage (III) During this stage of damage development, matrix cracks joined together, especially along ply interfaces, which caused delaminations between plies. The

delaminations usually grew in the plane of the laminate. In addition to transverse cracks and the crack coupling, longitudinal cracks were also present. These cracks, growing parallel to the load direction (0°) in the 0° plies, were present in Stage (II) but were few in number and short in length. They exhibited a fatigue character on a microscopic scale, growing slowly and stably with the increasing cycles. In fact, when a crack grows, it creates an interlaminar tensile normal stress which will tend to separate the plies, and an interlaminar shear stress which tends to shear the plies along their interface in the neighborhood of the crack. These two stress components provide the basis for a mechanism of crack coupling, longitudinal crack growth and delamination. These are illustrated in Figure 20 by the replica of an edge-damage (matrix crack and delamination) pattern recorded at a point near the middle of Stage (III) for Material W. This interfacial growth and crack coupling was the first distinctive feature of microdamage which separated fatigue damage from quasi-static loading damage, as it was not observed under static loading.

In Stage (II), matrix cracking was identified as the primary damage mechanism. In Stage (III), crack coupling, longitudinal cracks and interface separation (delamination and debonding) mechanisms seem to dominate damage development. The internal stress redistribution associated with this type of damage is characterized, in part, by the diagram in Figure

21. When the cracks in the off-axis plies grow along the ply interfaces and join other cracks, ply separation will occur, and the 0° plies must then act under completely uniaxial stress in this local delaminated region. The delaminated off-axis plies will carry no 0° load and will not constrain any lateral motion in the 0° plies. In that situation, the uniaxial stress in the 0° plies becomes the only load-bearing stress in the laminate. If such a stress situation occurs in the laminate, it will cause a corresponding reduction in stiffness. Crack coupling and (local) delamination or debonding (even in the interior of a specimen) near matrix cracks are viable strength or stiffness reduction mechanisms for the long-term fatigue behavior of composite laminates.

In Stage (III), whitening on the specimen surface was also observed. This is apparently fiber/matrix debonding. As more cycles were applied, more whitening occurred until the damage visible on the specimen surface was fairly uniform. Under uniaxial tension-tension cyclic loading, cyclic shear stresses are induced in the triaxial laminates, cyclic shear stresses cause whitening, thereby degrading the in-plane lamina shear modulus, which in turn leads to the loss in laminate stiffness.

It was also found that there was no difference in the matrix crack density between outer layers and interior layers (see Figure 13(a)).

Stage (IV) During this stage, damage propagated unsteadily in the composite. Evidence of this is demonstrated in Figure 19. In this figure the normalized axis stiffness as a function of the number of cycles of tensile fatigue loading for two cyclic stress levels is shown. A rapid, large decrease in stiffness in Stage (IV) was observed in one test. Both curves show the same generic shape suggested by the "damage development" curve in Figure 13. For a cyclic stress level of 15000 psi, the initial drop in elastic modulus corresponded to a 90° crack (CDS) formation which changes the laminate modulus. For a cyclic stress level of 12500 psi, the change in laminate modulus for matrix crack formation was very small. This result indicated that the specimen tested under the higher cyclic stress developed much more damage than that tested under the lower cyclic stress prior to final failure.

For laminates of Material W which were fatigue-loaded with a maximum cyclic stress amplitude of 12500 and 15000 psi for a long period of time, the drop of the final elastic modulus, E_f, was less than 15 percent prior to failure for both maximum stress levels as shown in Figure 19. This indicates that there was relatively little fatigue damage prior to failure and that the fracture was a rapid process once initiated.

Figure 19 shows a sharp drop in stiffness quite near the end of the test which apparently involved fiber fracture events. In fact, fiber fracture occurred throughout both

Stages (III) and (IV) [45]. Final failure and, it appears, those events immediately preceding failure, were dominated by 0° fiber failure. Two major modes of fiber failure were observed.

From the side view of the specimen, there was a distinct fiber failure sequence which began in Stages (III) and (IV). Figure 22(a) is an edge replica of this damage pattern. The interior section of a specimen cycled at 35% of its ultimate strength for about 85% of its life. In the Figure 22(a), the black horizontal line is a matrix crack in the ±45° layer, and the black spot in the 0° layer is a fiber break. Figure 22(b) shows some of the fiber fractures at a higher magnification. The black vertical line along the fiber in the photograph is debonding between the fiber and matrix interface. These specimens were polished slightly into the interior after cycling.

The second mode of fiber fracture was in the laminate interior. When the matrix cracks intersected at an adjacent ply or matrix cracks intersected fibers in the layer during fatigue loading, a series of local ply delaminations developed, and cracks (or debonds) developed along the fibers in the adjacent plies or in the layer. Then fiber fracture occurred. It was found that fiber fractures were sometimes associated with this damage mode. Fiber failures occurred in isolated random locations. An example is given in Figure 23, which shows debonding along a fiber near a matrix crack in a

45° layer.

The final event in Stage (IV) is the complete fracture of the laminate. Not all aspects of cumulative long-term fatigue-related fractures were clear.

In summary, fatigue damage development in the $[0°/\pm45°]_4$ laminate type can be characterized as follows: In Stage(I), no damage occurred; in Stage (II), the dominant mode was off-axis ply cracking; in Stage (III), transverse cracking development was complete. Longitudinal cracking and delaminations grew along the edges and across the width at the 0°/±45° and +45°/-45° interfaces; in Stage (IV), delamination growth continued until a substantial portion of the interfaces were delaminated at specimen failure (see Figure 24).

Fatigue Failure Criterion

Secant Modulus Criterion (Current Strain)

The secant modulus failure criterion [18] is applied to the triaxial laminate data in this section. This criterion states that the laminate will fail when the secant modulus (at current strain) is reduced to the range of the static secant modulus at static failure. Two static sequential loading-unloading tests were performed on Material V to determine a static secant modulus. Two specimens were tested to 95% of their respective average lifetime under fatigue loading at maximum stress levels of 12500 and 15000 psi. The specimens

were then loaded in tension to the same stress level as the maximum fatigue stress, and unloaded to observe further changes in secant modulus. In all cases, the frequency of fatigue loading was 15 Hz. This loading procedure is shown schematically in Figure 4. In this Figure, E_o represents the initial elastic modulus and E_s represents the static secant modulus. Therefore,

$$E_{sn} = \frac{\sigma_{max}}{\epsilon(n)} \qquad (4)$$

where,

E_{sn}: secant modulus at nth loading cycle

$\epsilon_{(n)}$: current strain at nth cycle (at maximum load)

σ_{max}.: maximum applied stress

Figure 24 shows the change in the secant modulus with fatigue cycles for two applied maximum stress levels. The static secant modulus at static failure is shown by the dotted line, and is not approached by the cyclic data at failure. The results in Figure 24 indicate that when a laminate failure occurred, the fatigue secant modulus (Figure 5) was far above the range of the static secant modulus at failure for both of applied cyclic stress levels. The fatigue secant modulus would clearly never decrease to within the range of the static secant modulus prediction prior to failure. Therefore, the secant modulus criterion is not valid for this application of triaxial glass fiber composites.

Cumulative Secant Modulus Criterion (Cumulative Strain)

The cumulative secant modulus concept is shown in the Figure 5. Figure 5(a) shows the hysteresis loop diagrams for triaxial laminates to determine the static secant modulus and cumulative fatigue secant modulus. To determine the static secant modulus, the specimen was initially loaded to ten percent of its ultimate strength and unloaded. Then the specimen was reloaded to forty percent of the ultimate strength and unloaded. The stress was increased in steps until the maximum stress was ninety-five percent of the ultimate tensile strength. The differences in slope was evidence that the ±45° plies failed (or matrix cracking occurred) in a progressive manner. To determine the cumulative fatigue secant modulus, the cyclic loading was interrupted during the cycling. Then, the specimen was loaded statically to the maximum cyclic stress level and unloaded. The cumulative fatigue secant modulus was recorded from this static loop and a stress-strain curve was generated. Referring to Figure 5(b), there are many definitions for stiffness and/or modulus, *e.g.* the initial stiffness, E_o, and the cumulative fatigue secant modulus, $E(n)$ (defined as the applied stress level divided by the corresponding cumulative strain at the nth loading cycle, $\epsilon(n)$.

$$E(n) = \frac{\sigma_{max.}}{\epsilon(n)} \qquad (5)$$

where,

$E(n)$: cumulative fatigue secant modulus at nth loading cycle

$\epsilon(n)$: cumulative strain at nth loading cycle

σ_{max}: applied maximum stress

Figure 25 shows the change in the cumulative fatigue secant modulus with fatigue cycles for two applied maximum stress levels. The static secant modulus at static failure is shown by the dotted line. The result shown in the Figure 25 shows that when laminate failure occurred, the cumulative fatigue secant modulus was lower than the cumulative secant modulus prediction for the both applied cyclic stress levels. Therefore, the cumulative secant modulus criterion could be used as the fatigue failure criterion for the glass fiber triaxial laminates. Other verification of this criterion for other loading conditions and materials is required.

Edge Effects

Wrapped and unwrapped edge triaxial laminate, Materials T, U, V and W, were fatigue tested at a stress ratio, R = 0.1. In these cases, the frequency of fatigue loading was varied inversely with the stress level to keep a constant loading rate. Materials T and W had the same reinforcement, T had wrapped edges as shown in Figure 7, while W specimen were machined from sheets in the usual manner to prepare coupons. Similarly, Materials U and V had the same reinforcement with

U having wrapped edge and V machined edge. Difficulty was encounter in measuring the initial elastic stiffness for T and U due to the irregular edge surfaces.

Fatigue Resistance

As mentioned in Chapter Two, questions had been raised as to whether or not the wrapped and unwrapped edge laminates would exhibit differences in fatigue resistance which would be evident in the *S-N* curve (or fatigue lifetime curve). In fact, it was found that the existence of an edge effect is very dependant of the maximum cyclic stress level. Figure 27 and 28 present the fatigue results in the form of *S-N* curves for Materials T, W, U and V, respectively. The fatigue data are compared with two theoretical trend lines. The linear trend follows the 10% static strength loss per decade of cycles which has been extensively reported for unidirectional glass fiber dominated composites [11], as discussed in Chapter 2. The data fall slightly below this line. The nonlinear curve was fit to the data with a least squares routine following Equation 3. This Equation describes the data well with an exponent, m = 11.56 for Materials T and W as shown in Figure 27, and m = 8.3 for Materials U and V in Figure 28. As noted in Chapter 2, a fit to Equation 3 implies a lifetime determined by a crack growth mechanism [1].

The results in Figures 28 and 29 indicate that, particularly in the high cycle region (or lower stress) there

was not much difference in the lifetime data for the wrapped or unwrapped laminates. It appeared that these two kinds of material systems degrade at about the same rate. Figure 29 shows a photograph of the fractured surfaces for the wrapped and unwrapped laminates which were subjected to the lower fatigue stress level (12500 psi). It indicates that the wrapped and unwrapped laminates had almost the same failure modes: both fracture surfaces were almost flat. Therefore, the difference in laminate fabrication between laminates did not affect the overall fatigue resistance. At higher cyclic stresses (or lower cycle number region), the wrapped and unwrapped laminates did have some small differences in the lifetime data as shown in Figures 27 and 28, but these still appear to be insignificant.

Effect of Triaxial Reinforcing Fabric Variations

Materials V and W had the same fiber and matrix materials, but the triaxial reinforcing fabrics had different stitching patterns. For Material V, the stitching yarns with which fiber layers (0/±45) were held together were oriented in a 90° direction with respect to the 0° fibers, while for Material W, the stitching yarns were oriented in a 0° or ±45° direction (see Figure 29). Because of the different stitching patterns, the fibers in Material V were packed much more closely and there was less matrix between fibers and a thinner

matrix layer between 0 and ±45 plies than those in Material W, as shown in the Figure 30(a) and (b).

As expected, the static stress-strain response of Material V was similar to that of Material W, shown in Figure 31. The initial elastic moduli were about 2.8×10^6 psi for both kinds of the laminate. The static mode of failure was typically extreme brooming of the fibers.

The following results of Materials W and V are compared to evaluate the effect of the stitching patterns.

Fatigue Resistance

The fatigue *S-N* data for Materials V and W, cycled at R = 0.1, are shown in Figure 32. Material W, which had the looser stitching pattern, shows significantly longer fatigue lifetime than Material V over the entire stress range. Data for both materials fell below the 10%/decade line, as is typical of triaxially reinforced laminates [1]. However, Material W showed the best fatigue resistance of any commercial triax system tested as part of the MSU program [1].

Damage Development

Materials V and W were fatigued at R = 0.1 and at maximum stress σ_m = 15000 psi to observe fatigue damage patterns. The un-normalized and normalized amount of fatigue damage in terms of its effect on elastic modulus are plotted versus cycles in Figures 33 and 34 respectively. In Figure 33, it appears that

Material V developed much more damage than Material W at the given stress level and cycles. The results in Figure 34 show that the elastic modulus dropped nearly twenty percent for Material W while the elastic modulus dropped only by nearly ten percent of the initial value for Material V before failure. These results indicate that Material W could accumulate much more fatigue damage than Material V prior to final failure.

From the micro-damage observation of Material V under fatigue loading, there were numerous delaminations and matrix cracking initiating and growing from the stitching which was oriented at 90° rather than from the 0° or 45° stitching (see Figure 35).

Fracture Surface

Examination of the fracture surfaces of the specimens which were subjected to fatigue tension-tension testing in the higher cycle region, Material W failed with jagged, irregular failure surfaces and Material V failed with a relatively smooth, straight failure surface. A photograph of typical failure modes for the two kinds of laminates with different stitching patterns is shown in Figure 36. Comparison of these two materials clearly shows the more damaging effect of laminates having tight stitching material in the 90° direction. The reasons can be expressed as follows: First, for Material V in which the stitching materials were all in the 90° direction, the layers were stitched tightly together,

preventing the formation of a polyester interlayer between the plies as shown in Figure 30(a) and (b). The analytical results from a finite element analysis [47] showed that the stresses in the high fiber region were higher than the stresses in the average fiber region and the presence of a matrix interlayer between plies played a significant role in reducing the stress concentration. Thus, the thinner the matrix layer between the fiber layers, the more stress concentration at the interface. Second, the fibers in Material V were also stitched tightly together within a strand, preventing the formation of a polyester matrix between the fibers. Due to being closely packed together, the fibers could not be wet out with matrix, which would cause more voids between the fibers and matrix. Thus, all these negative effects could reduce the interlaminar shear strength, in-plane shear properties and would finally reduce the fatigue resistance of the laminate.

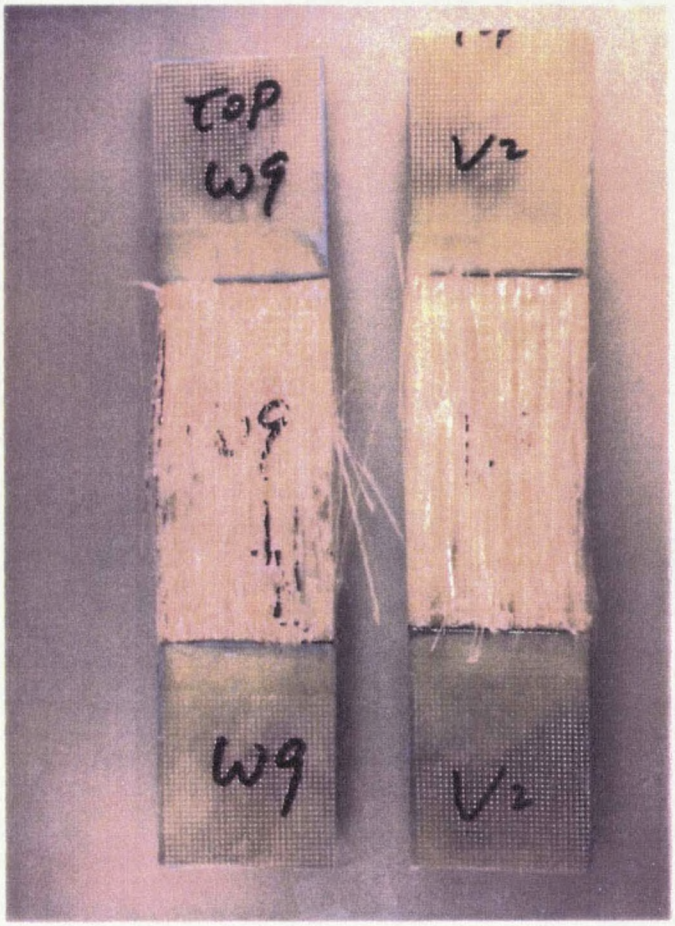

Figure 12. The $[0°/\pm45°]_4$ fractured specimens: (left) Material W and (right) Material V. Static Tests.

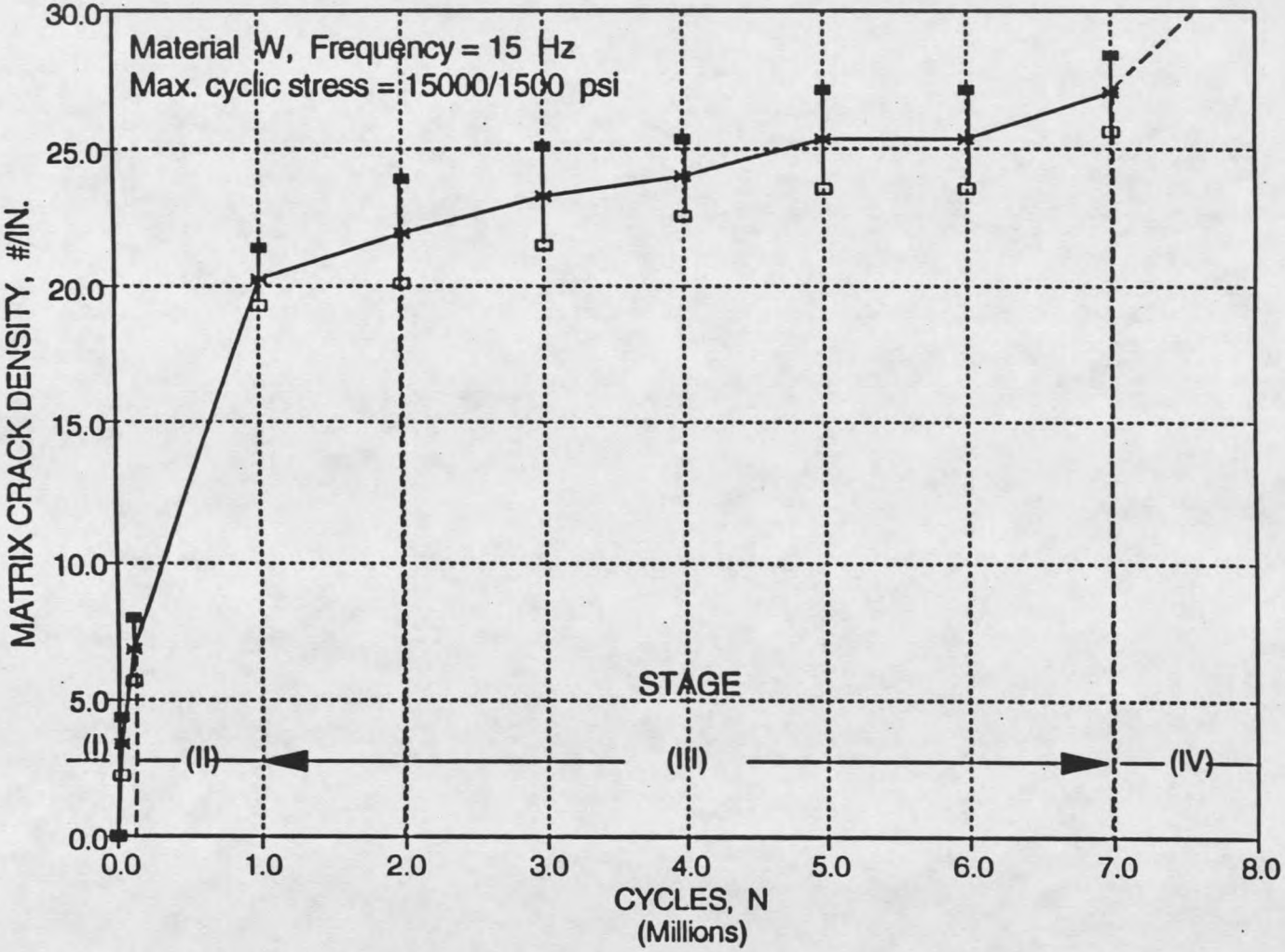

Figure 13. Typical damage development for a $[0°/\pm45°]_4$ laminate.

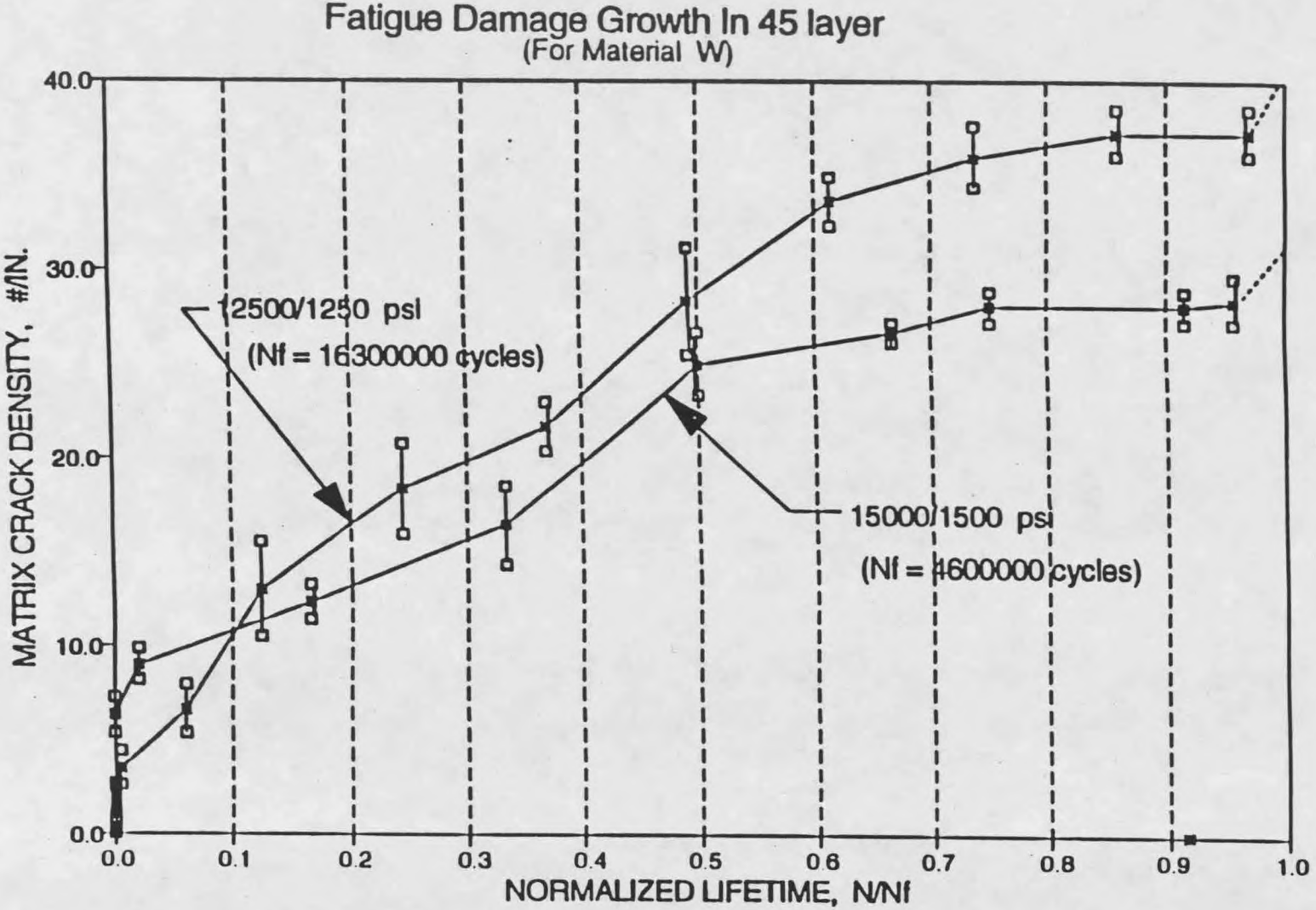

Figure 14. Damage growth of triaxial laminates subjected cyclic loading at two load levels.

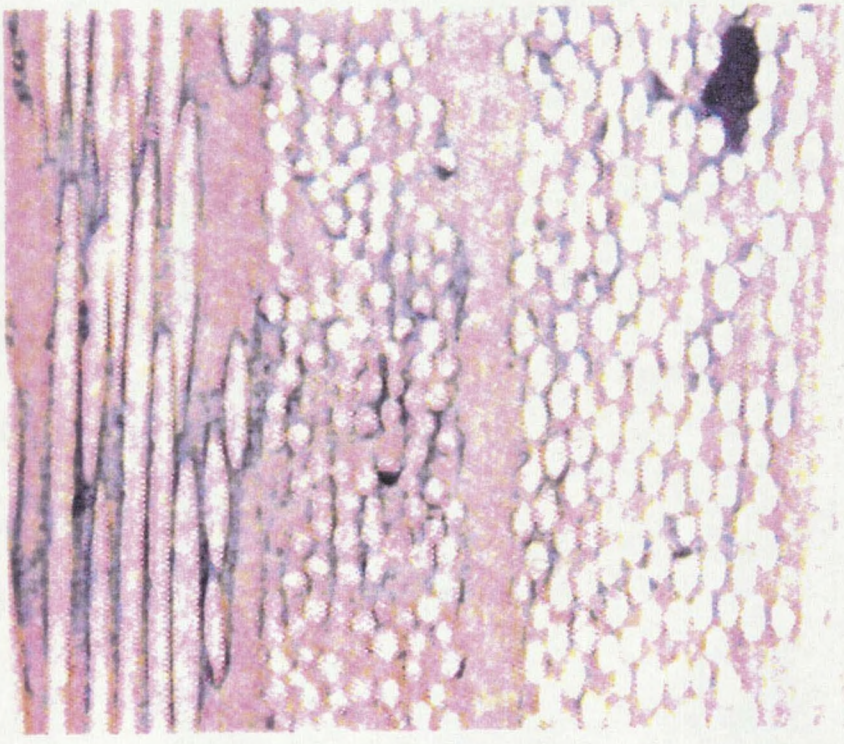

Figure 15. Edge replica from a $[0°/\pm45]_4$ laminate at stage (I).

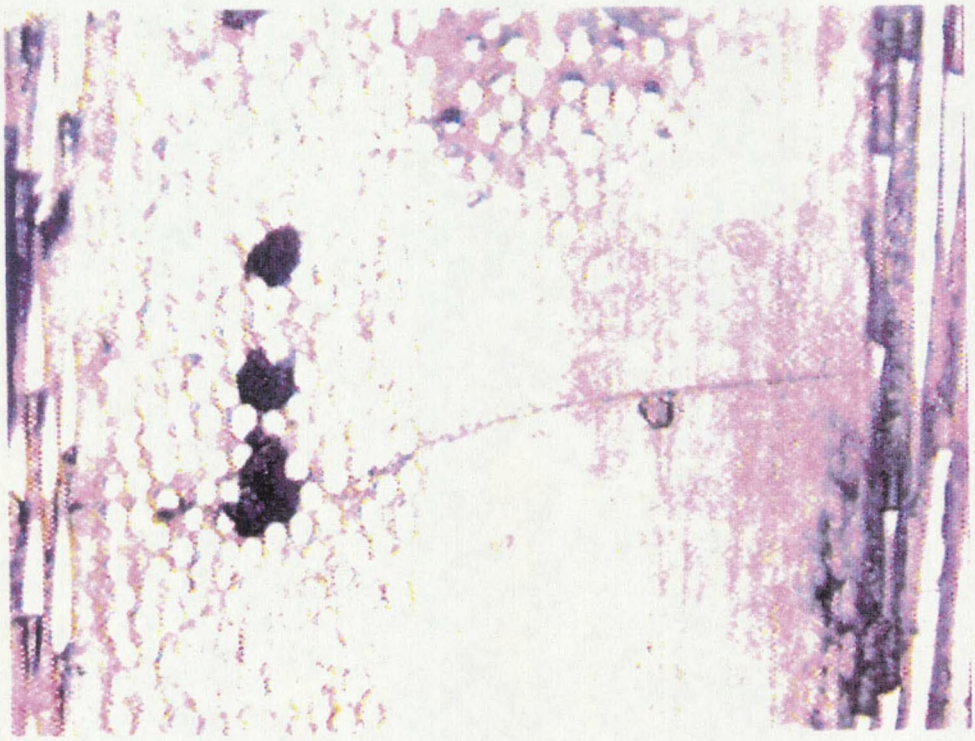

Figure 16(a). Edge replica from a $[0°/\pm45°]_4$ laminate at stage (II).

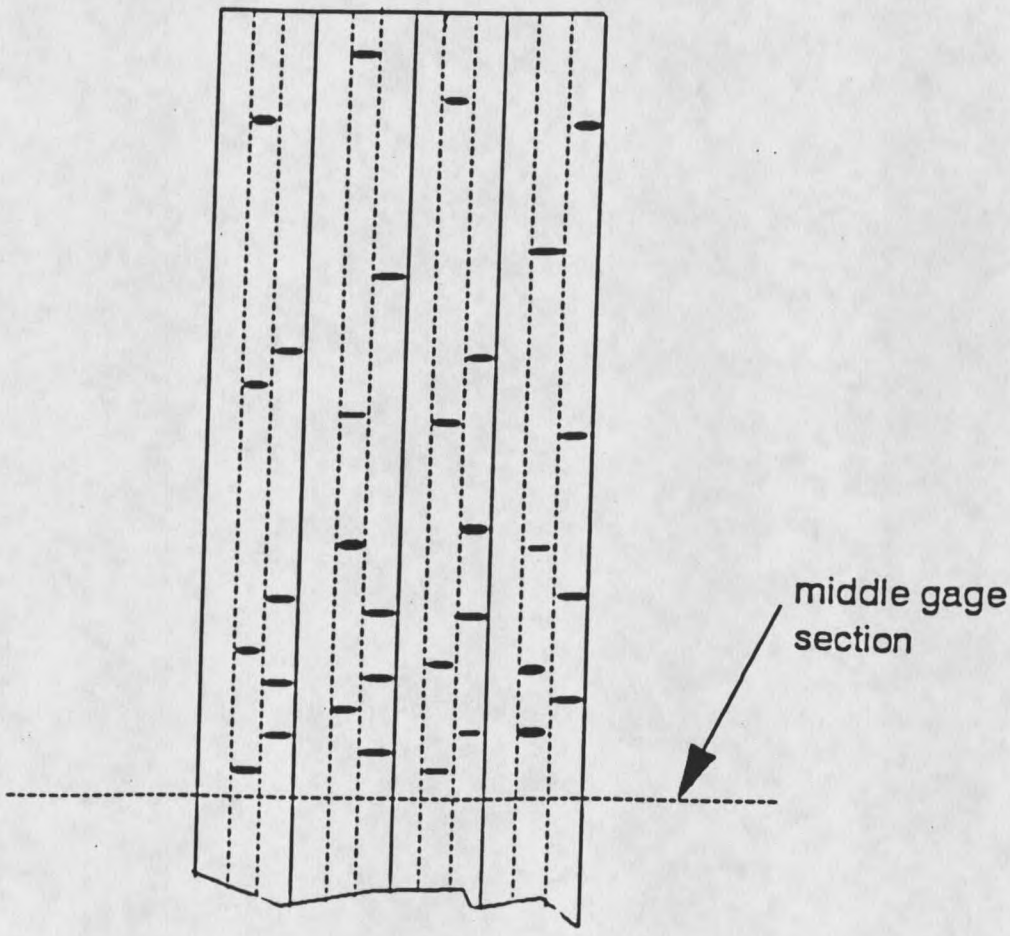

Figure 16(b). Schematic view of crack pattern along edge of specimen.

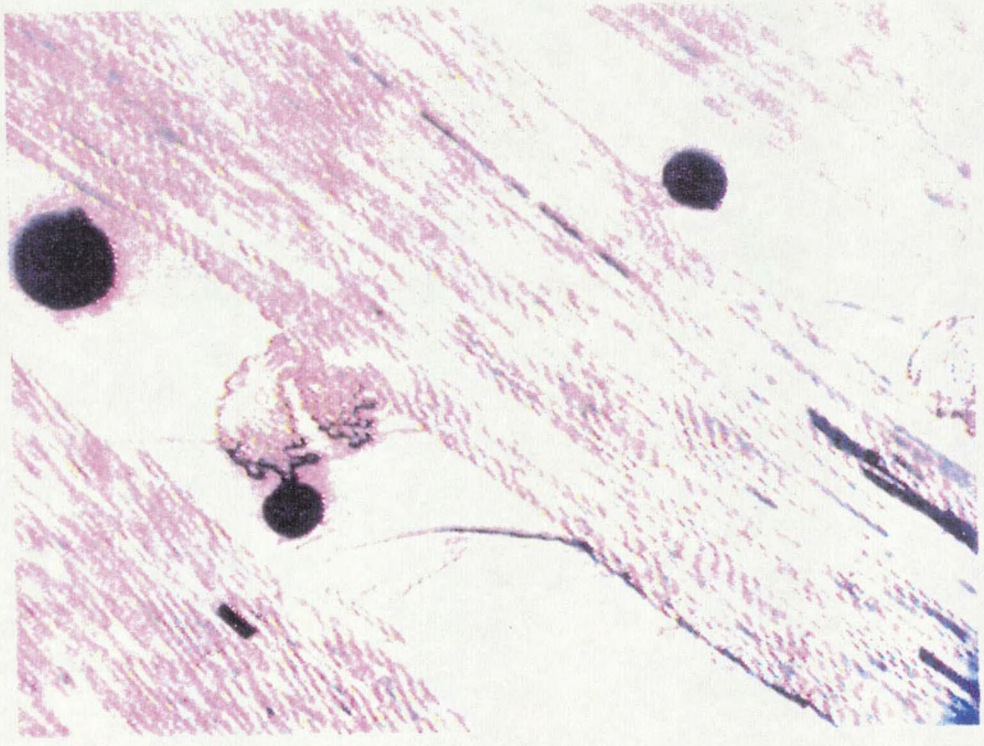

Figure 17. Cracks in interior section at Stage (II).

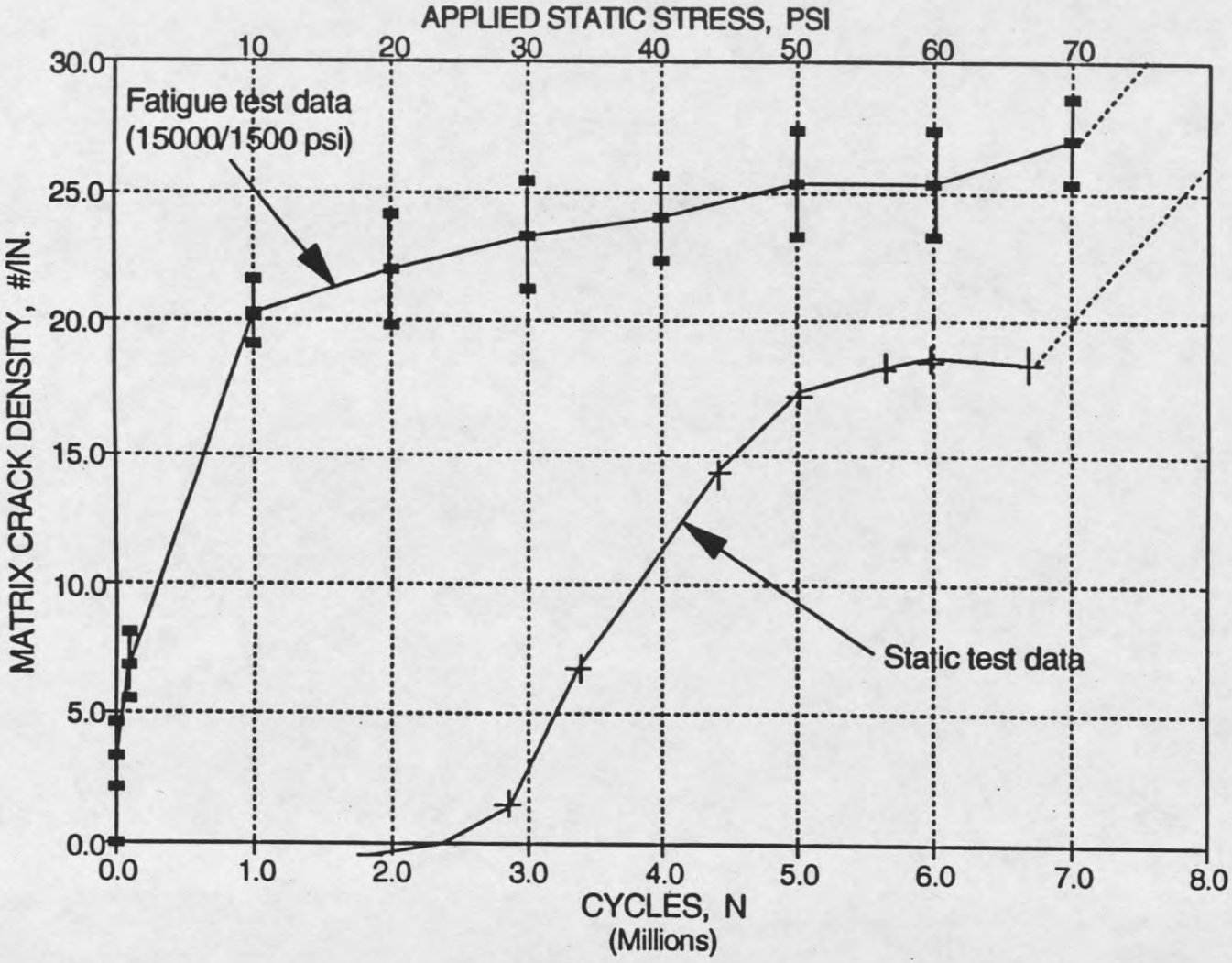

Figure 18. Damage growth for Material V subjected to cyclic loading (bottom scale) and static loading (top scale).

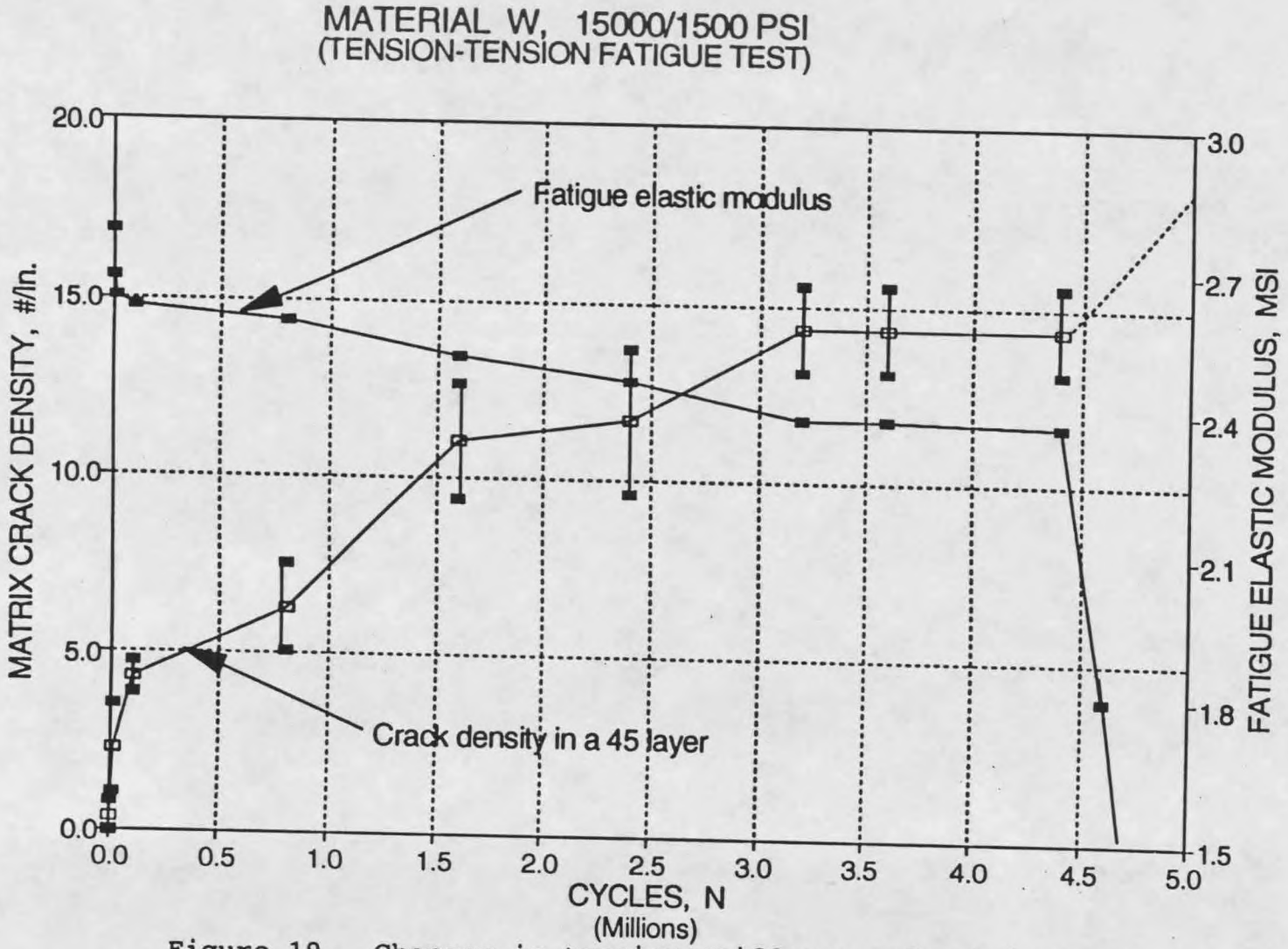

Figure 19. Changes in tension stiffness and matrix crack density as a function of cycles.

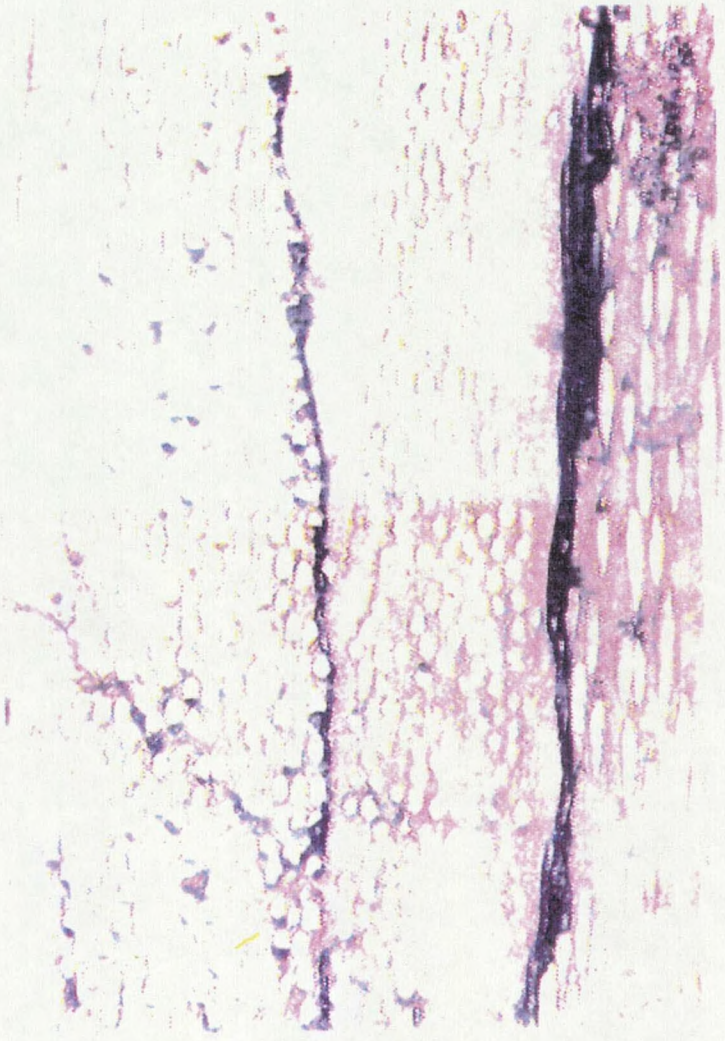

Figure 20. Edge replica from a $[0°/\pm45°]_4$ laminate in Stage (III).

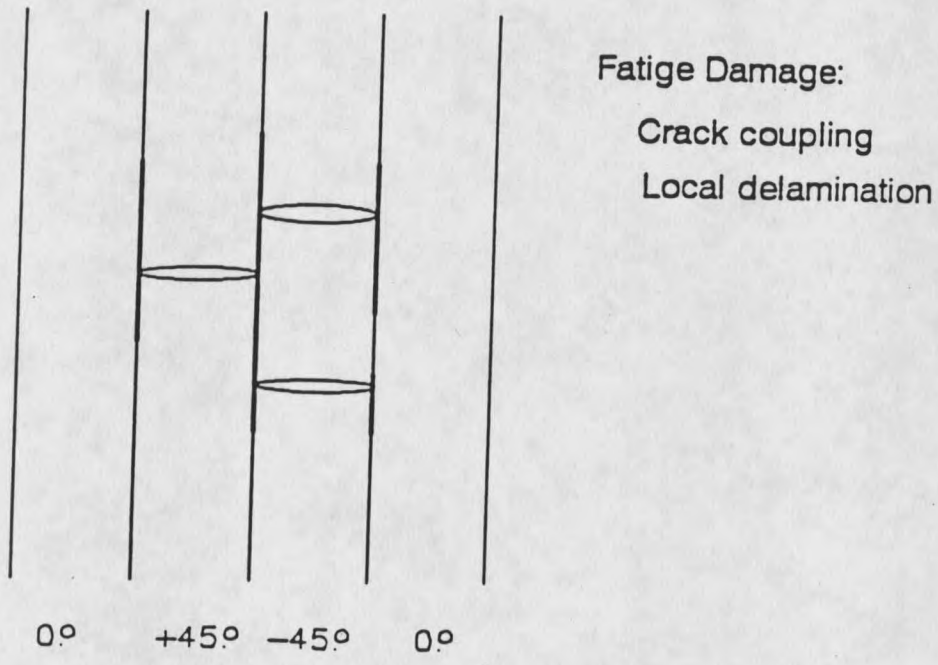

Figure 21. Schematic diagram of local region of influence for matrix cracking and local delamination.

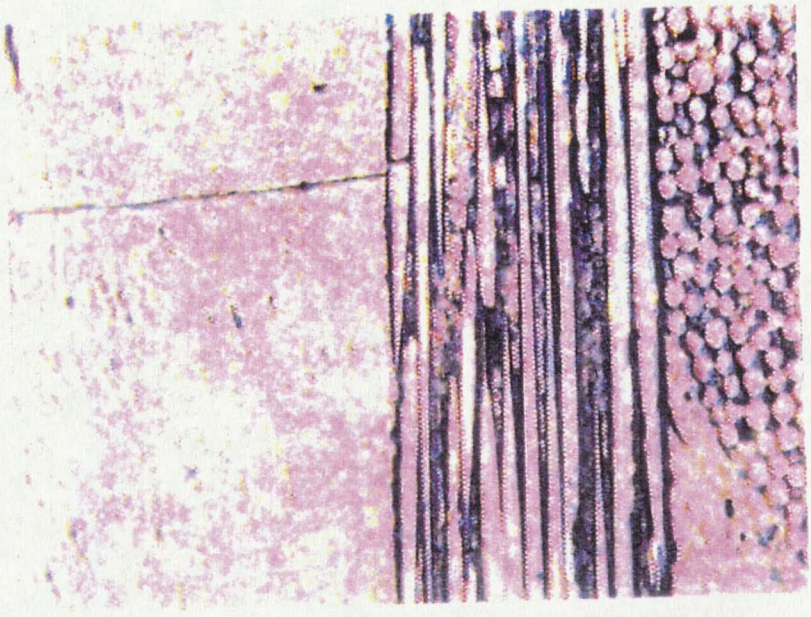

(a)

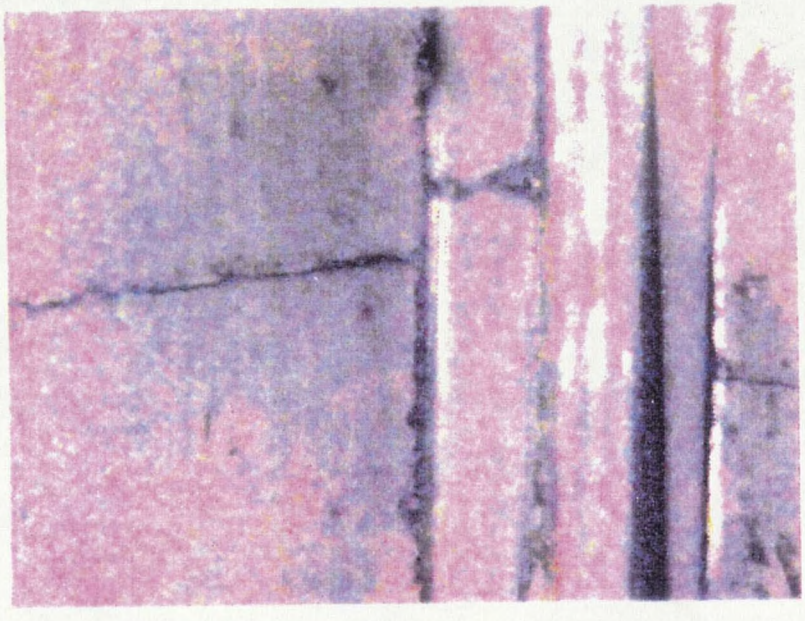

(b)

Figure 22. Edge views showing a fiber break for 85 percent of expected life(a) at magnification and (b) at high magnification. (Material W).

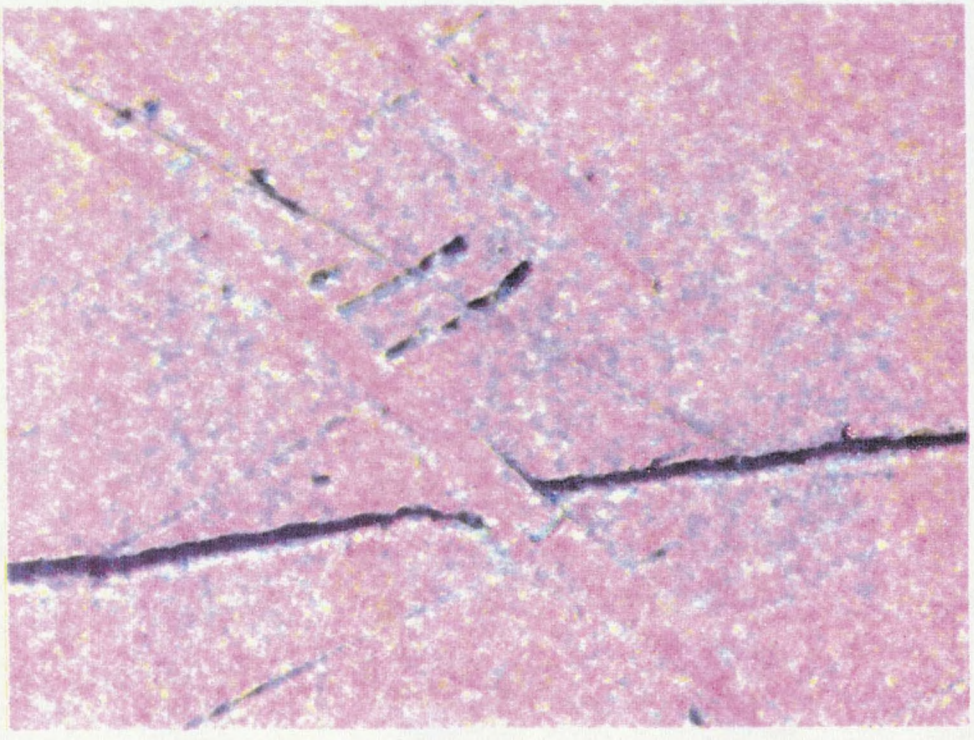

Figure 23. Edge view showing a 45° fiber break at Stage (IV).

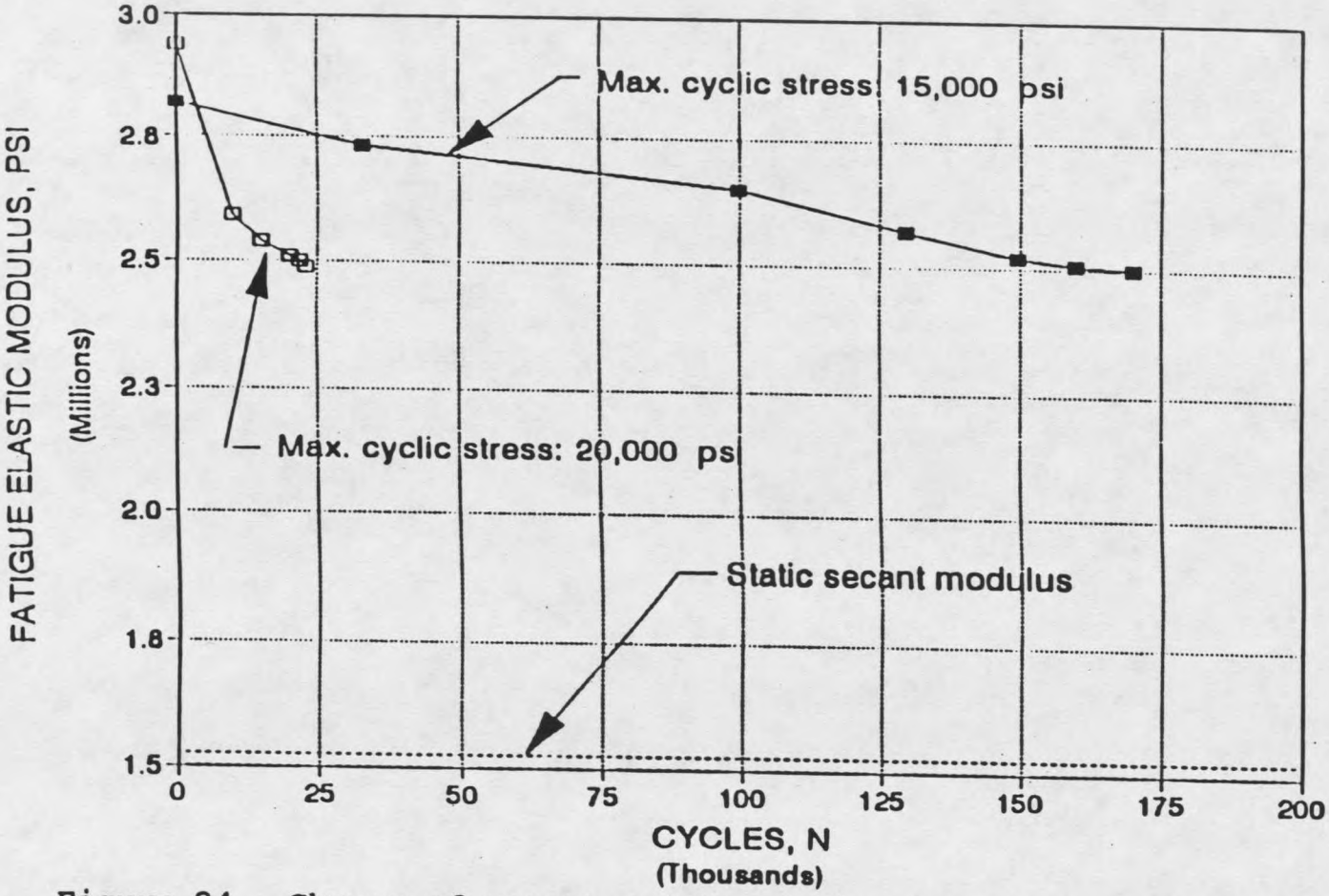

Figure 24. Change of secant modulus during fatigue. (Material V). Failure occurs when fatigue scant modulus is reduced to within the range of static secant modulus.

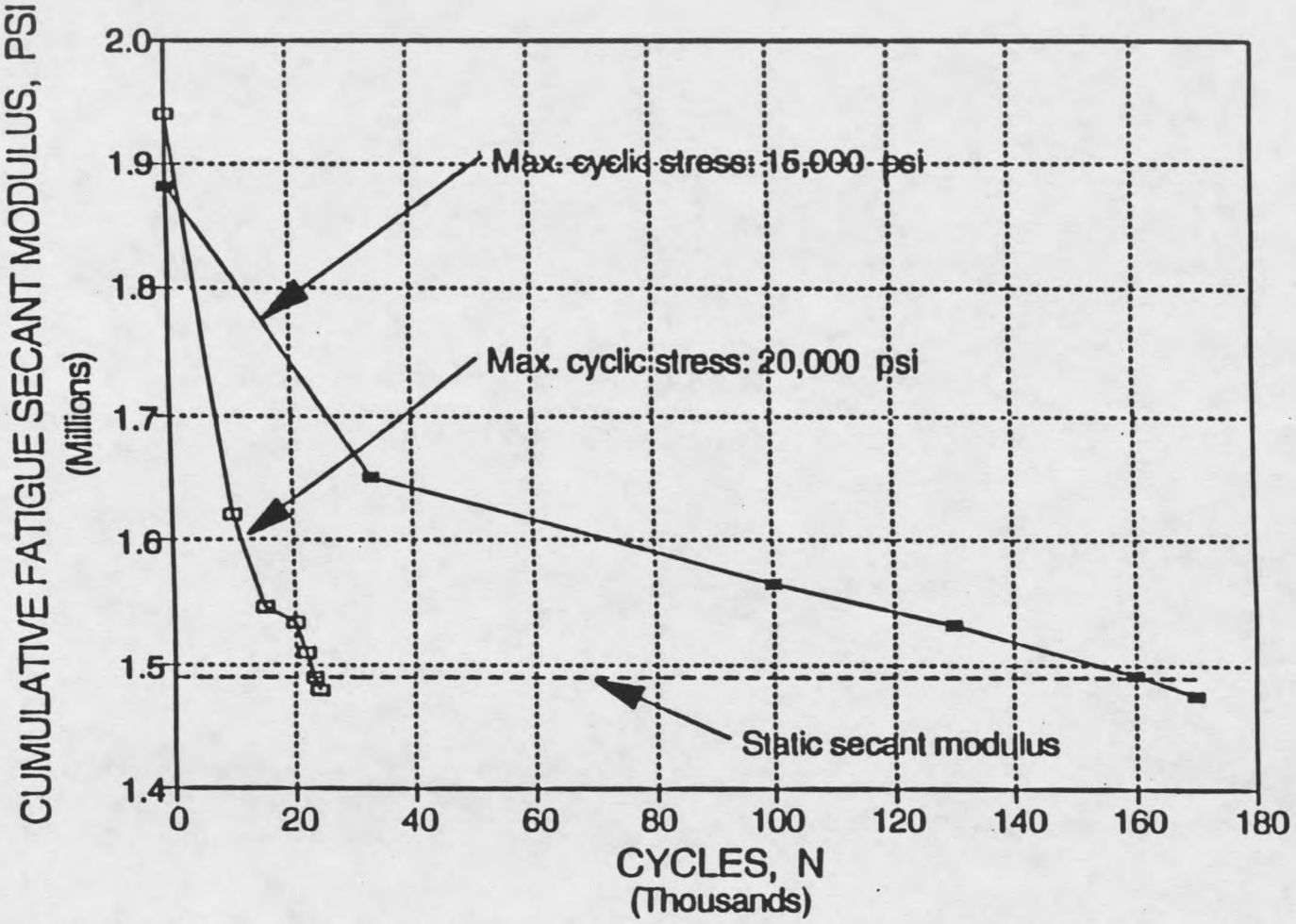

Figure 25. Change of cumulative fatigue secant modulus during fatigue. Failure occurs when cumulative fatigue secant modulus is reduced to within the range of modified static secant modulus. (Material V).

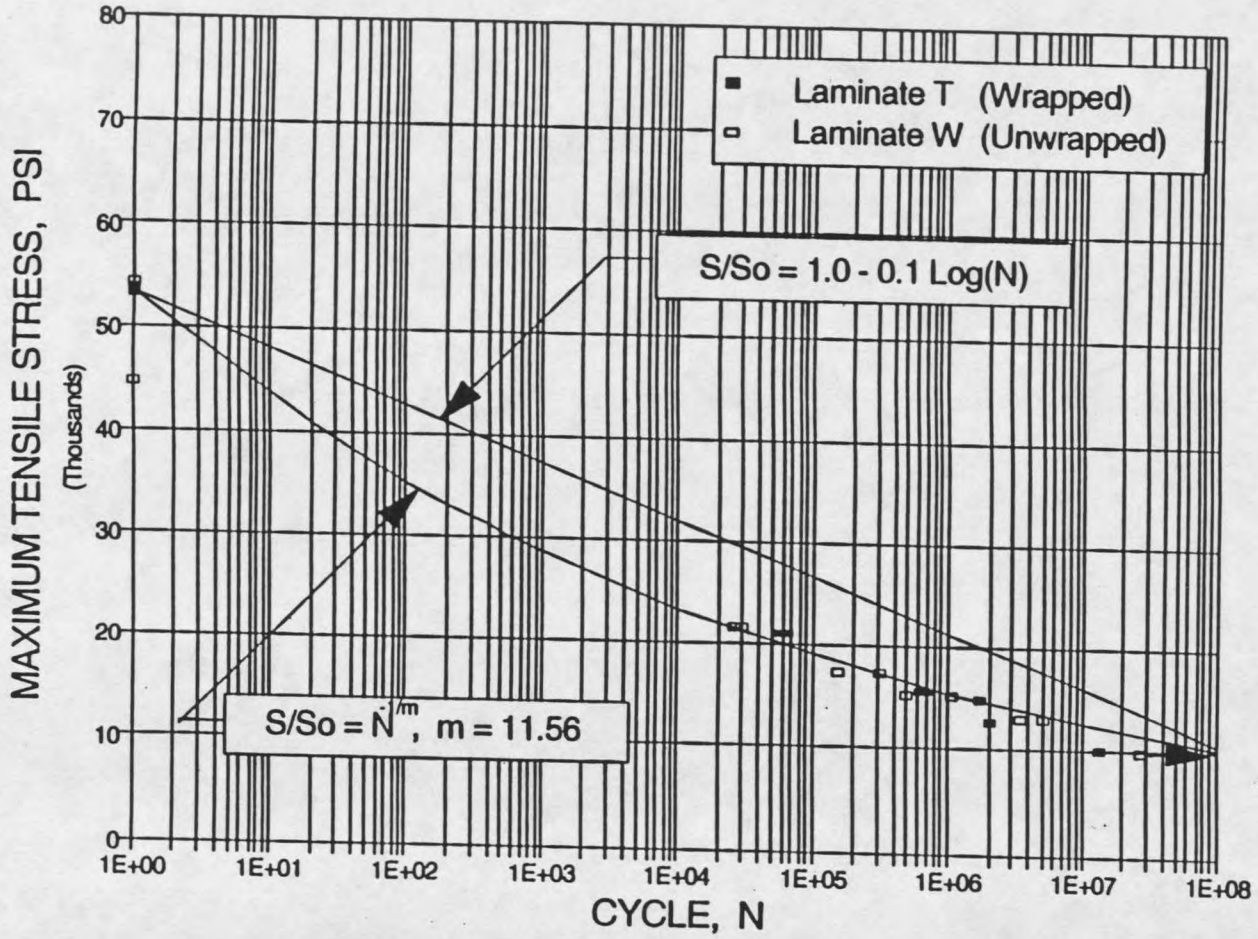

Figure 26. S-N curve for Materials T and W, triaxial glass/polyester, R =1, 1 to 15 Hz.

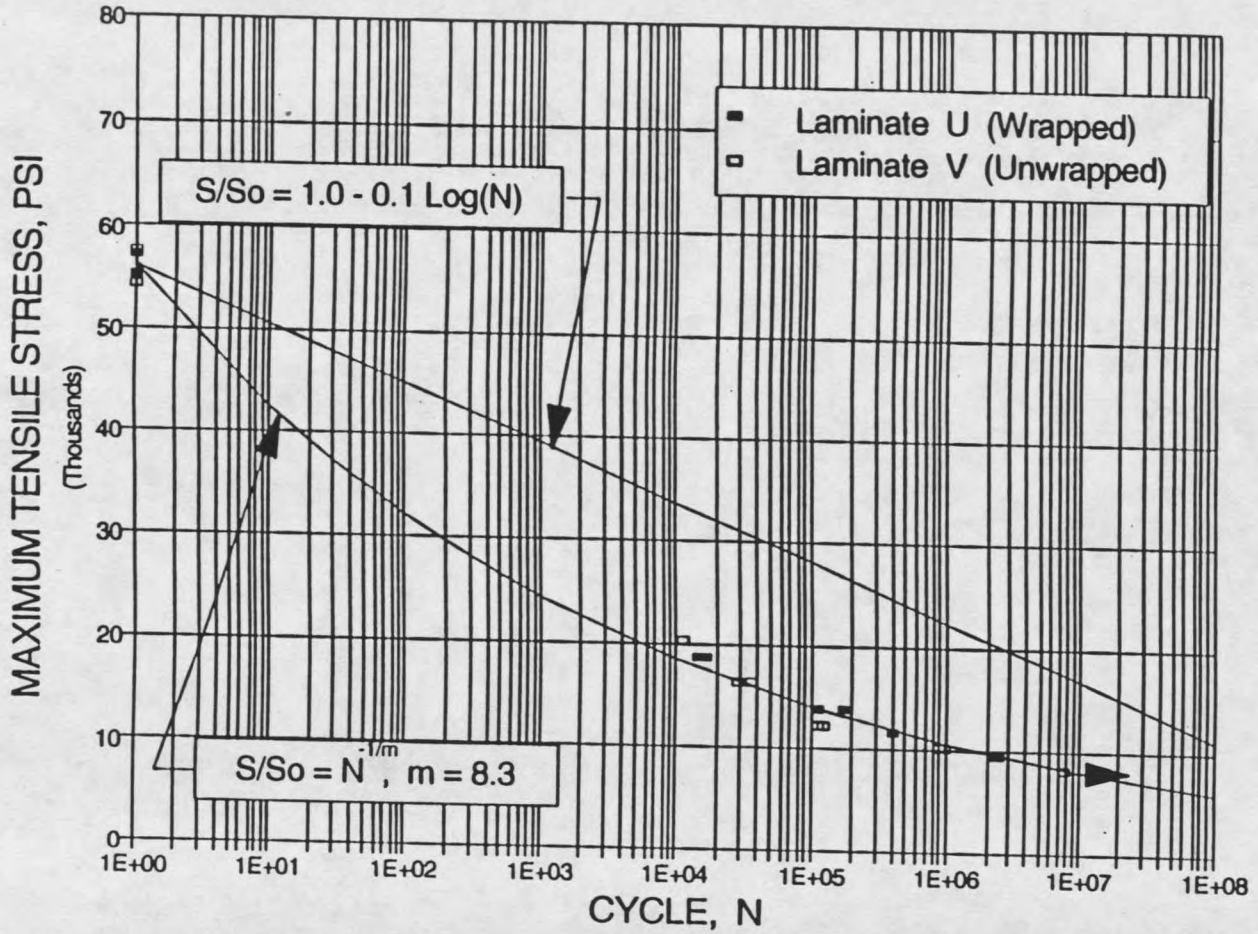

Figure 27. S-N curve for Materials U and V, triaxial glass/polyester, R = 0.1, 1 to 15 Hz.

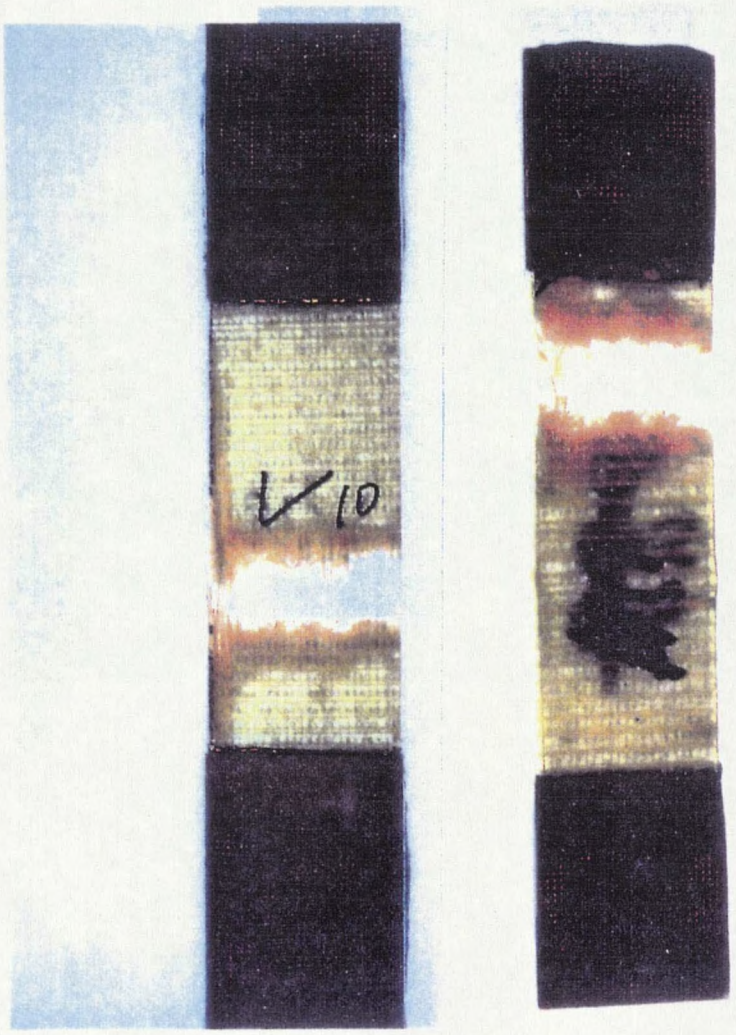

Figure 28. Fracture surface of wrapped and unwrapped laminates tested at lower cyclic stresses. (left) Material V and (right) Material U.

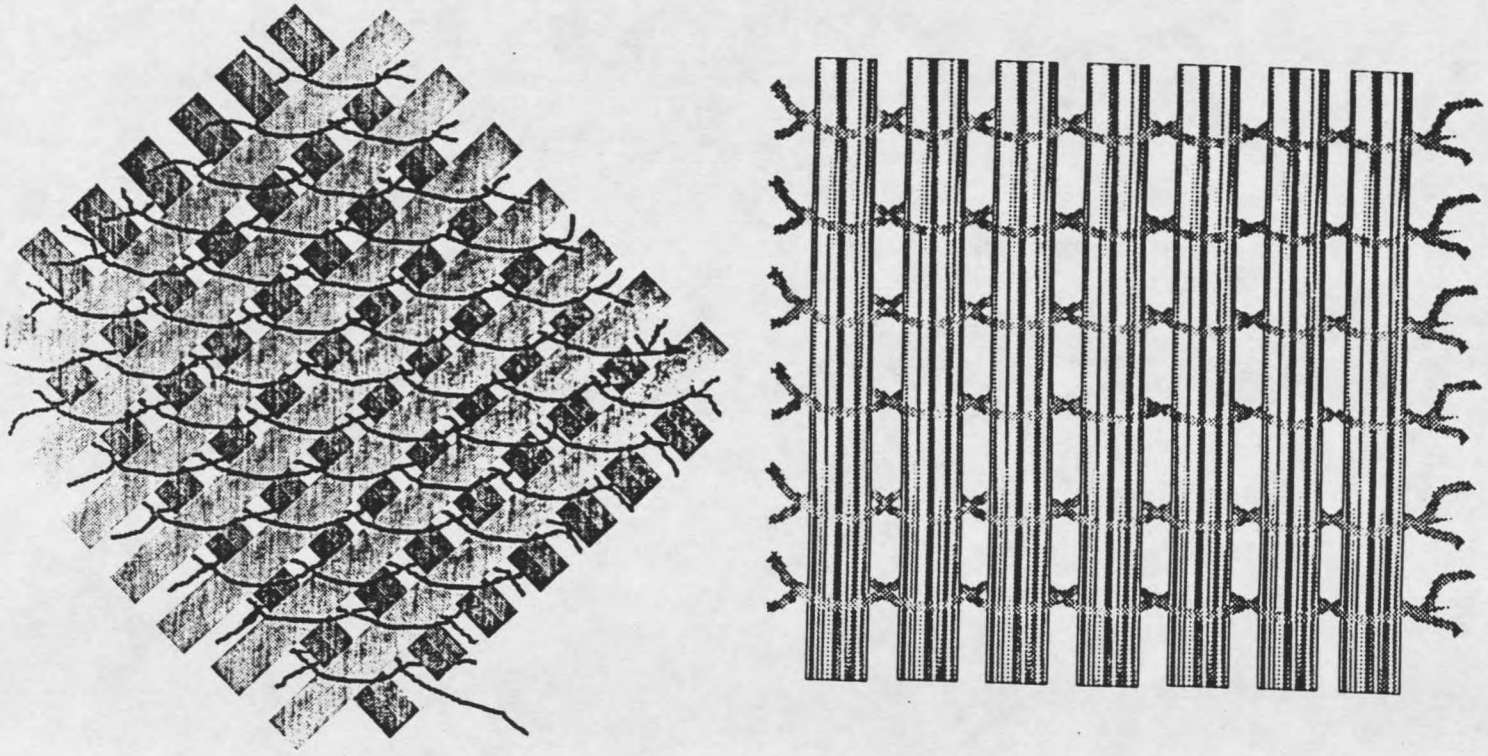

Figure 29(a) A stitching pattern for Material V.

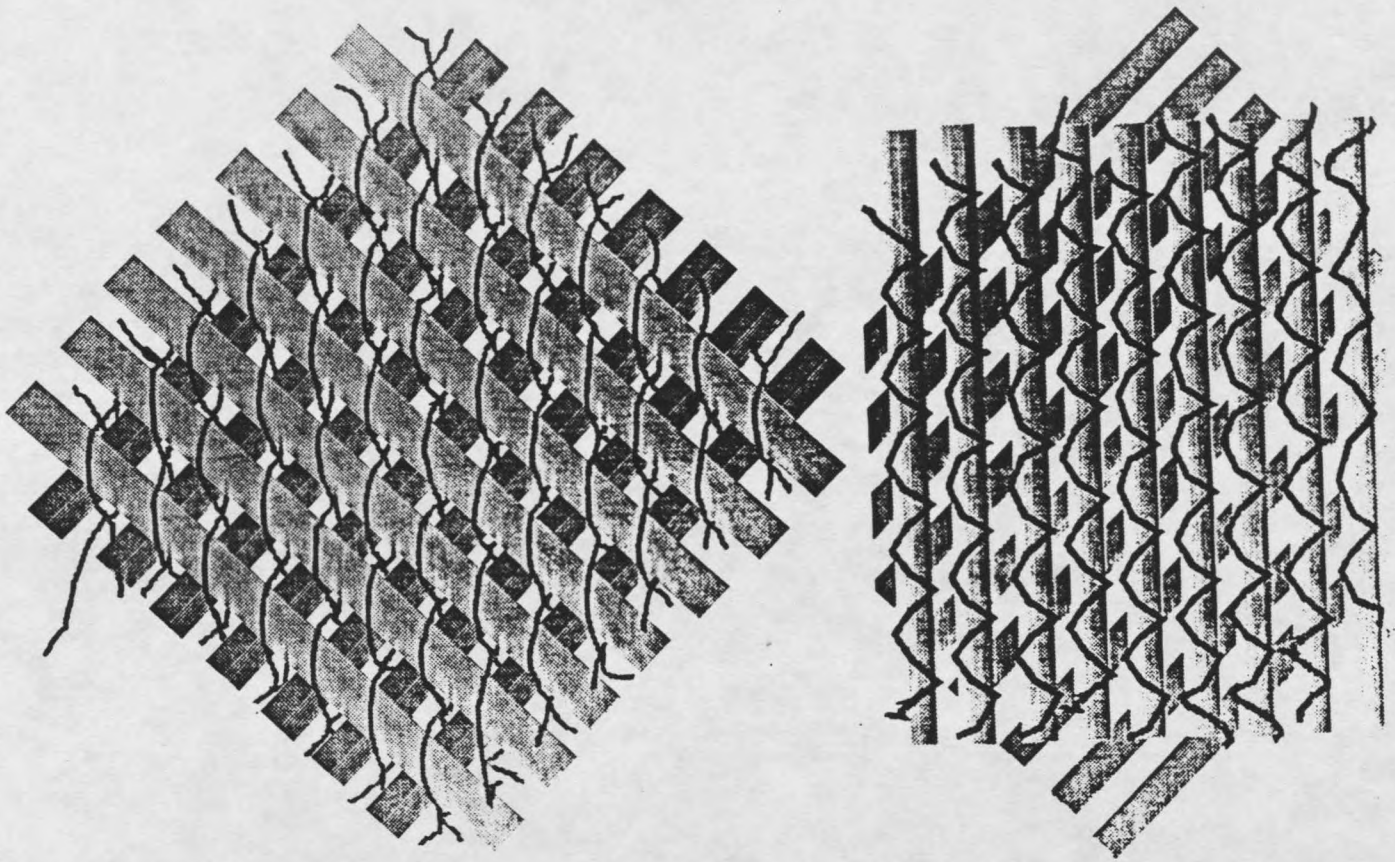

Figure 29(b) A stitching pattern for Material W.

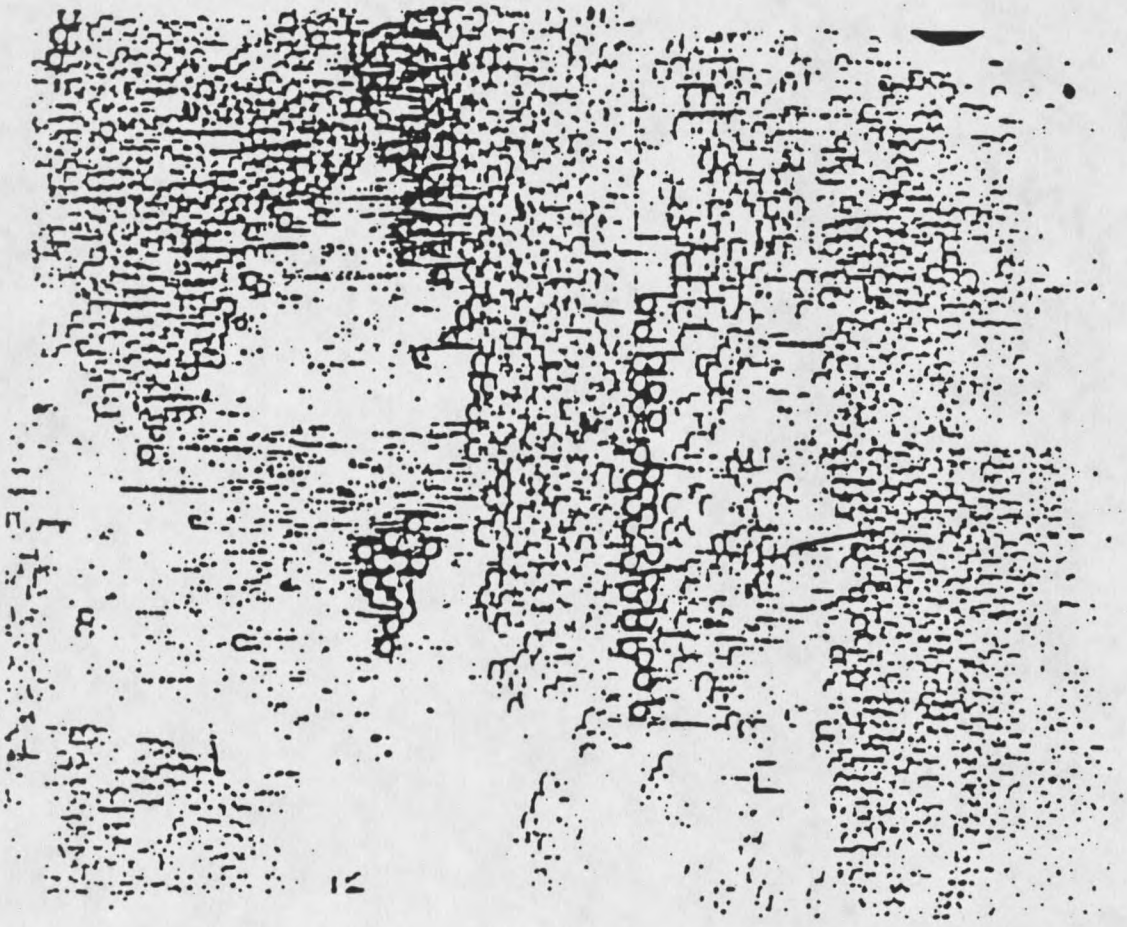

Figure 30(a). A cross-sectional view showing fiber distribution in Material W.

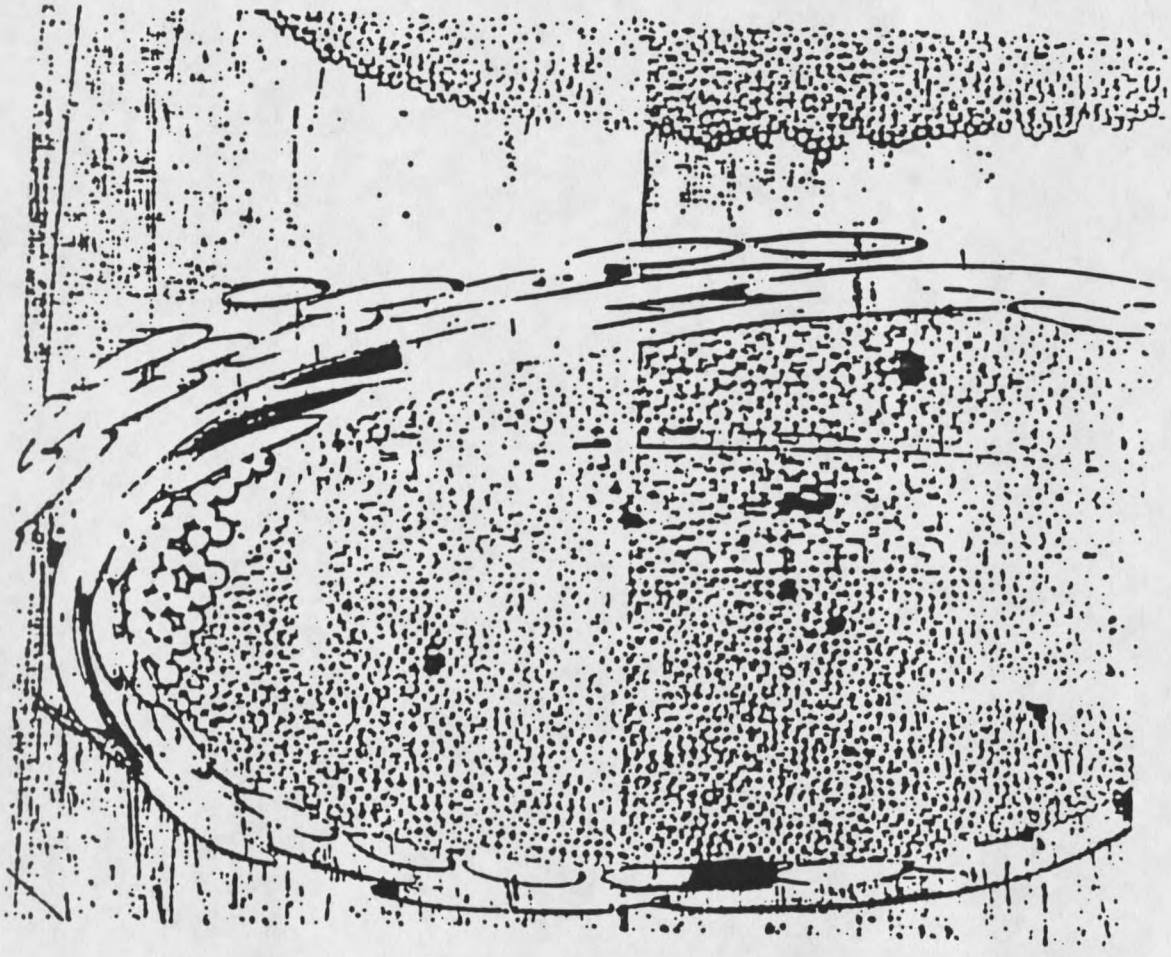

Figure 30(b). A cross-sectional view showing fiber distribution in Material V.

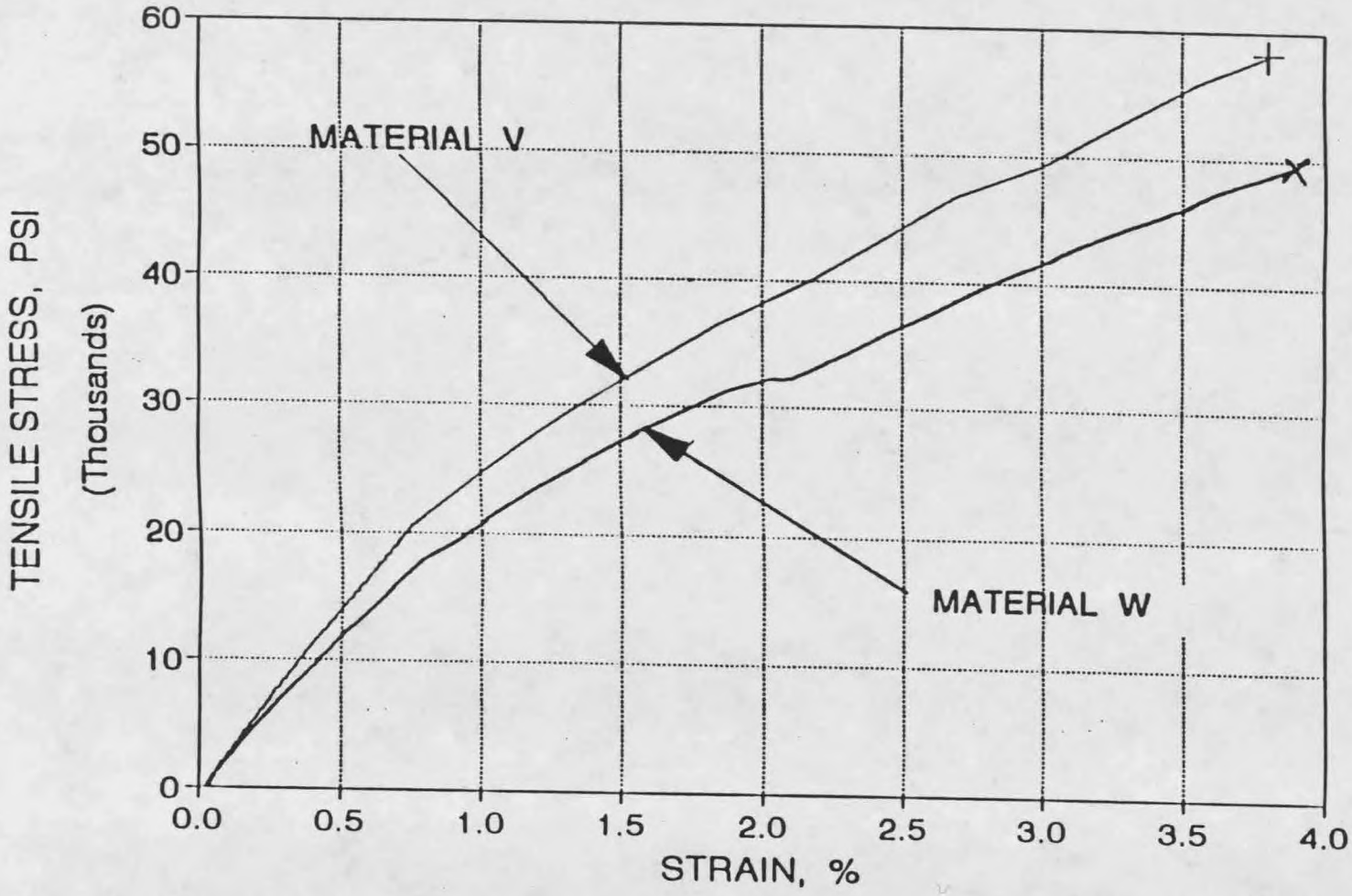

Figure 31. Stress-strain curves for Materials V and W.

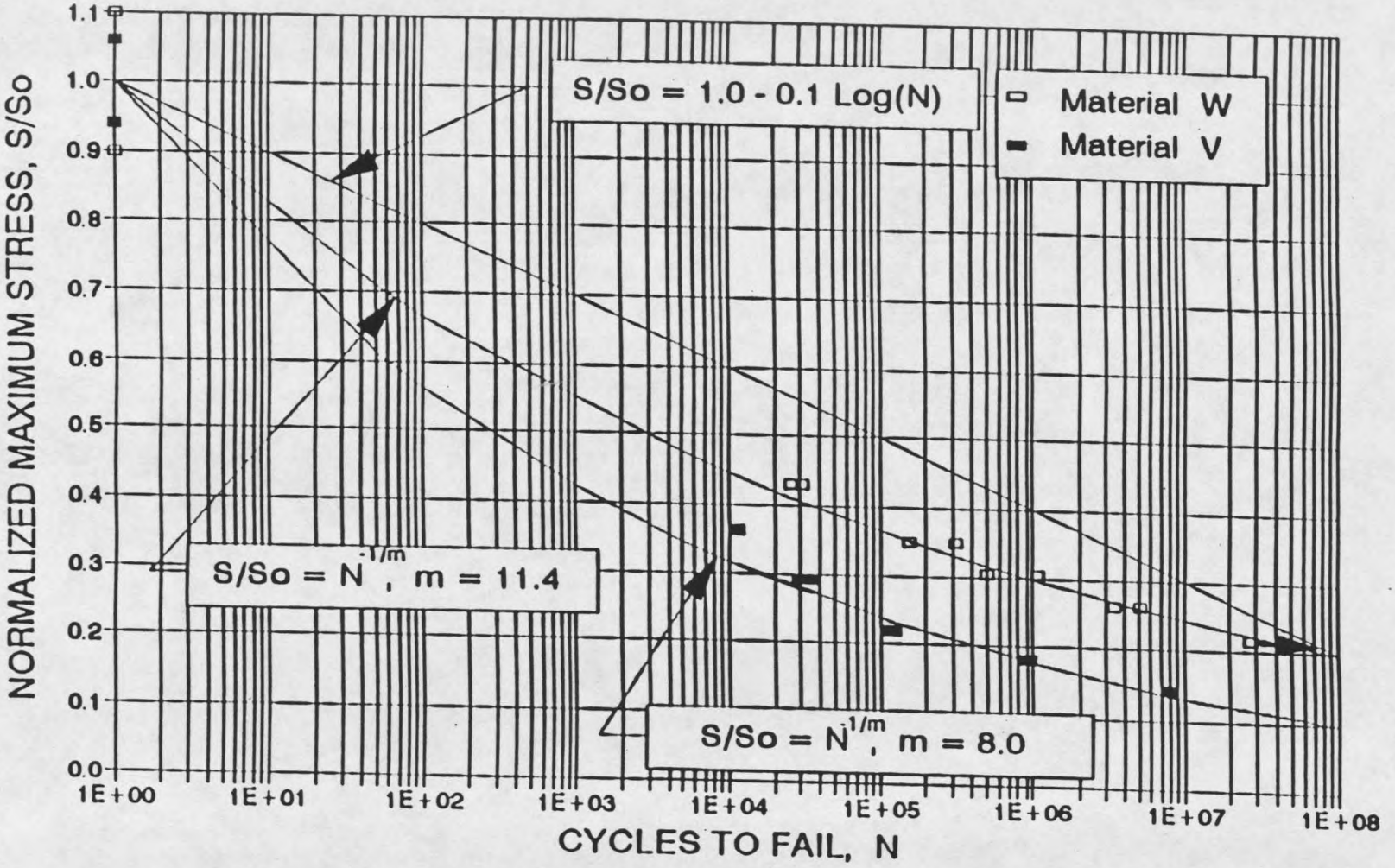

Figure 32. S-N curves for Materials V and W (standard coupon) with different stitching patterns.

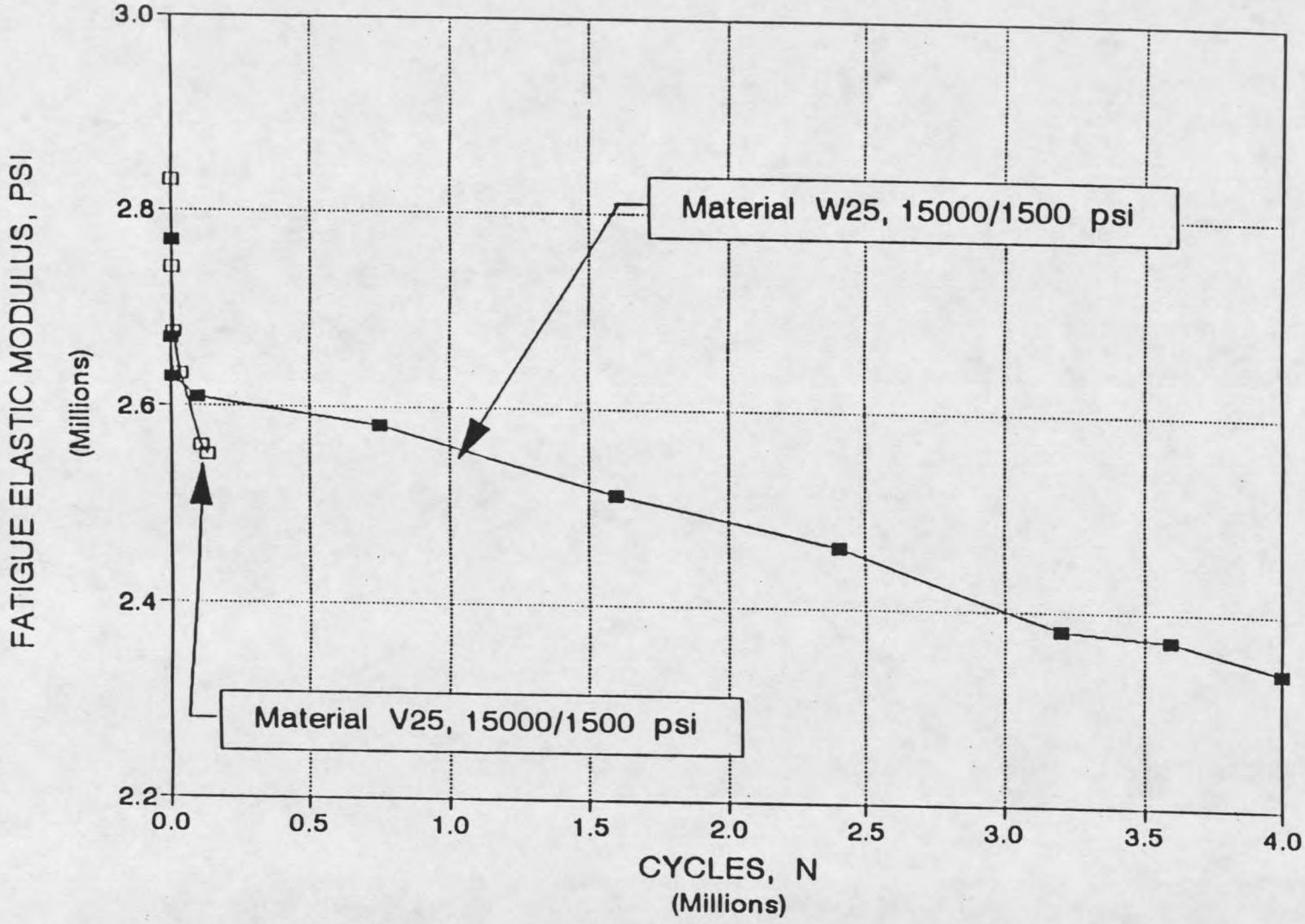

Figure 33. Stitching effects on fatigue damage growth and fatigue life for Materials V and W.

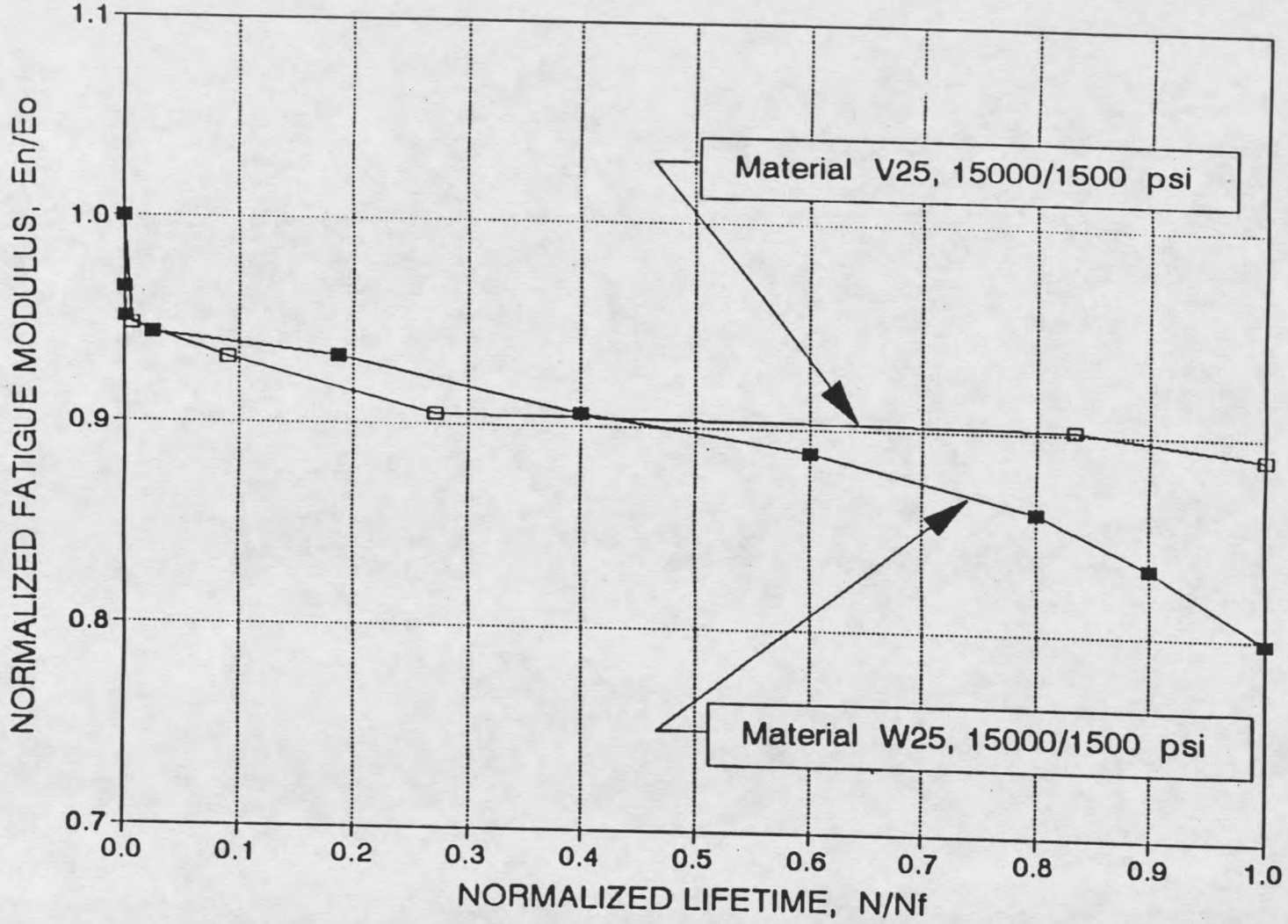

Figure 34. Stitching effects on normalized fatigue damage growth for Materials V and W.

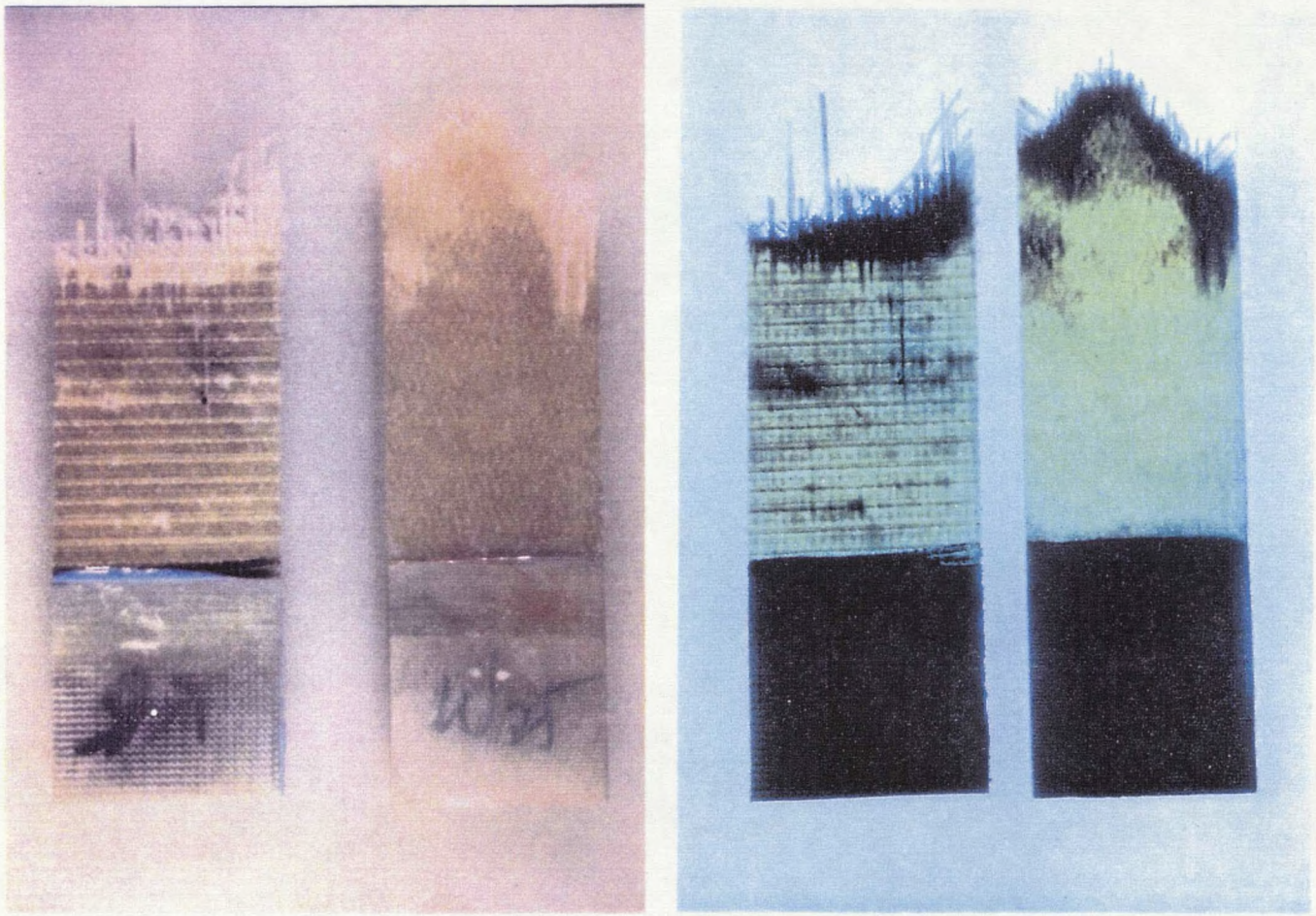

Figure 35. Damage initiation from the stitching material. Material W is on the right in each photo, Material V is on the left. (a) reflected light (b) transmitted light

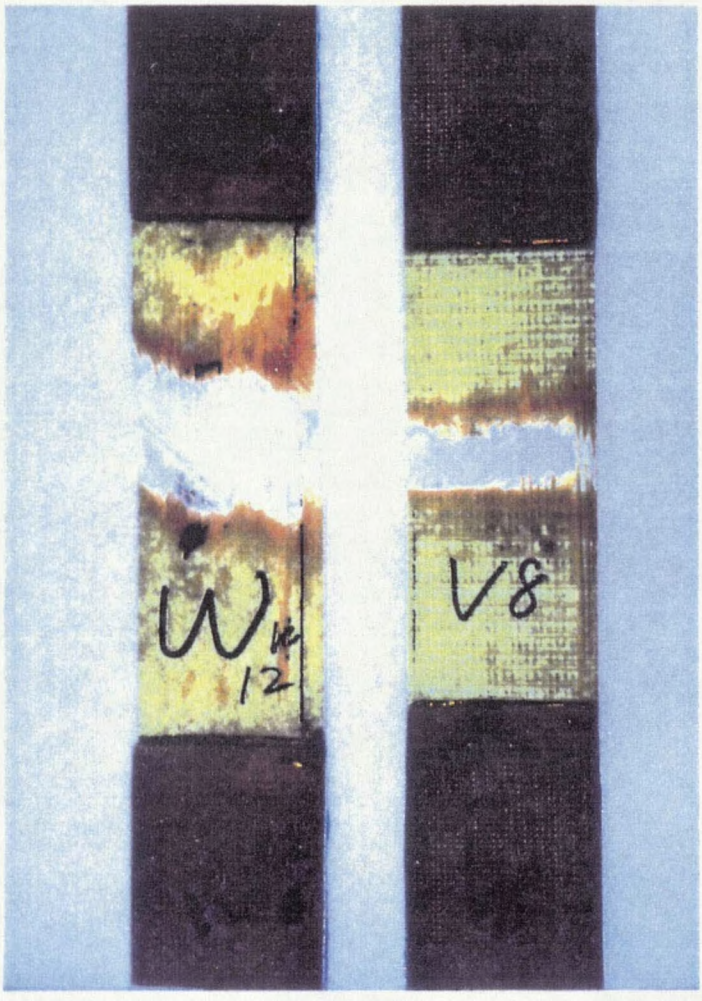

Figure 36. Stitching effects on fatigue fracture modes for Materials V and W.

CHAPTER FIVE

CONCLUSIONS AND RECOMMENDATIONS

Conclusions

One objective of this program was to isolate stiffness changes due to matrix cracking experimentally and to correlate the stiffness change with the damage growth. The residual modulus of long-life specimens showed a sharp reduction initially, followed by a more gradual decrease, then remained relatively unchanged until quite near 60% of their lifetime. The level of modulus reduction was stress dependent. A comparison of edge replicas of specimens subjected to quasi-static tension and tension-tension fatigue loading indicated that the saturation damage state was independent of loading history. Identical damage states were formed under high static stresses and repeated cycles at lower stress levels. The extent of damage accumulation and stiffness reduction was found to depend on the applied cyclic stress level and on the number of load cycles. The details of the results of this investigation are potentially valuable as the basis for suggesting generic aspects of damage development during long-term fatigue loading of composite laminates of the type

tested.

This study also showed a distinct response of glass/polyester $[0°/\pm45°]_4$ composite laminates to moderate and high cycles: no damage at low cycles; damage accumulation caused primarily by growth of matrix crack in the off-axis plies at moderate to high cycles; and localized failure of the fibers at high cycles. Extensive fiber failure was the final event in laminate fracture. The matrix cracks in the laminate do not appear to cause fiber failures directly. This is consistent with reported findings for other classes of composites.

The extent of damage accumulation measured in terms of the axial elastic stiffness reduction and matrix crack density, was found to depend on the applied cyclic stress level and on the number of load cycles.

Matrix cracking initiated near the middle section of the gage length and then progressed toward the tab section of the coupons with cycles during the fatigue testing or increasing the stress level during static testing. These composite laminates also developed more fatigue damage near the middle section of the gage length than at other sections of the gage length. This pattern was independent of the loading history whether the laminates were tested at different stress level, static loading, or fatigue loading conditions. There was no difference in the rate and mode of damage development between the outer plies and interior plies in a composite laminate.

The secant modulus criterion did not accurately predict the fatigue failure of this type of composite laminate, because the degradation of fatigue secant modulus did not exceed the degradation of the secant modulus prediction prior to failure. A modified fatigue modulus criterion was tested and proven that it predicted the fatigue failure of the $[0°/\pm45°]_4$ laminates very well.

Fatigue tests were also performed on laminates which had different coupon edge condition. Results of these tests indicate that unwrapped edges had only minor effects on lifetime as compared with coupons fabricated with specially wrapped edges. Thus, fatigue data from coupon tests should be applicable to composite structures which do not contain machined (free) edges.

The effects of reinforcing fabric variations on the long-term fatigue behavior were also studied. Data on material lifetime were obtained at a series of stress levels. Different stitching patterns did affect the fatigue behavior of the laminates. The laminate in which stitching was sewn loosely in 0° and 45° directions into the fiber layers, had a much longer fatigue lifetime than the laminate in which stitching was sewn tightly in the 90° direction. The reason is that for Material V, the layers were stitched tightly together, preventing the formation of a polyester interlayer between the plies. The presence of a polyester interlayer between plies plays a significant role in reducing the stress

concentration, as indicated by a finite element model. However, the different stitching patterns produced no significant change in static strength.

Recommendations

The results of the few variable amplitude tests presented in Chapter 4 indicate that the damage accumulation mechanism is load history (*e.g.* maximum stress level) independent. Further testing with the full range of maximum stress levels and understanding are required in this area such that fiberglass composites can be properly designed to withstand the random loadings that are very much a part of the real world applications.

The secant modulus failure criterion would be different from material to material. A general modulus failure law could be established through experimental research on different materials.

Additional fatigue tests on different types of triaxially reinforced laminates (such as laminates with different stacking sequence, thickness, orientation and fiber content), and fatigue tests at lower and higher stress levels could be done to clarify whether wrapped edges have effects on the fatigue properties of the laminates during the overall fatigue life, since our study considered only two reinforcement cases. Future research work concerning the free-edge reinforcement concept is suggested. These suggestions are classified as

either theoretical or experimental, although any further research should combine elements of both. That is, any theoretical studies should be experimentally verified, and any experimental studies should be extended by suitable theoretical work in order to attain results of design significance. A logical follow-up to this work would be a more comprehensive experimental program dealing with different laminates and wrapping technique designs.

The experimental results from the study of reinforced fabric variations showed that different stitching patterns had a very significant effect on the fatigue properties of the fiberglass composites. Laminates in which stitching materials are sewed loosely in 0° and ±45° directions could potentially be used on the long term high cycle tests. However, these experimental studies should be theoretically confirmed through two or three-dimensional finite element analysis with the correspond model of different stitching patterns. Both experimental and analytical studies could then provide information on the relative improvement in fatigue resistance. The best performance appears to come from laminates with no stitching of 0° to ±45° materials, but the limits of stitching effects have not been explored. Stitching is very useful for material handling and fiber orientation control during fabrication, but much looser stitching might be adequate for those purposes.

REFERENCES

1. Mandell, J.F., "Fatigue of Fiber glass Wind Turbine Blade Materials," Contractor Report SAND92-7005, Sandia National Laboratories, Albuquerque, N.M., 1992.

2. Charewicz, A. and Daniel, I.M., "Damage Mechanisms and Accumulation in Graphite/Epoxy Laminates", *Composite Materials: Fatigue and Fracture, ASTM STP 907*, Hahn, H.T. Ed., American Society for Testing and Materials, Philadelphia, pp. 274-297, 1986.

3. Brostow, W. and Coneliussen, R., *Failure of Plastics*, Hanser Publishers, Munich, 1986.

4. Johnson, W.S., Ph.D thesis, Duke University, 1979.

5. Masters, J.E. and Reifsnider, K.L., "An Investigation of Cumulative Damage Development in Quasi-Isotropic Graphite/Epoxy Laminates", *Damage in Composite Materials, ASTM STP 775*, Reifsnider, K.L. Ed., American Society for Testing and Materials, Philadelphia, PA, pp. 40-62, 1982.

6. Reifsnider, K.L., "Damage and Damage Mechanics", *Fatigue of Composite Materials*, Reifsnider, K.L. ed., Elsevier Science Publishers, New York, pp. 11-75, 1990.

7. Sun, C.T. and Jen, K.C., "On the Effect of Matrix Cracks on Laminate Strength", *Journal of Reinforced Plastics and Composites*, Vol 6, pp. 208-222, 1987.

8. Lafarie-Frenot, M.C. and Henaff-Gardin, C., "Formation and Growth of 90° Ply Fatigue Cracks in Carbon/Epoxy Laminates", *Journal of Composites Science and Technology*, Vol. 40, pp. 307-324, 1991.

9. Herakovich, C.T., "Failure modes and damage accumulation in laminated composites with free edges", *Journal of Composites Science and Technology*, Vol. 36, pp. 105-119, 1989.

10. Dharan, C.K.H., "Fatigue Failure Mechanisms in a Unidirectional Reinforced Composite Material", *Fatigue of Composite Materials, ASTM STP 569*, American Society for Testing and Materials, pp. 171-188, 1975.

11. Mandell, J.F, Huang, D.D. and McGarry, F.J., "Tensile Fatigue Performance of Glass Fiber Dominated Composites", *Composites Technology Review*, Vol.3, pp. 96, 1981.

12. Mandell, J.F., "Fatigue Behavior of Short Fiber Composite Materials", Chapter 9 of *The Fatigue Behavior of Composite Materials*, Reifsnider, K.L. Ed., Vol. 4, Elsevier Science Publishing, London, 1991.

13. Mandell, J.F., Reed, R.M., Samborsky, D.D. and Pan, R.Q., "Fatigue Performance of Wind Turbine Blade Composite Materials", Contractor Report SED-Vol. 14, Sandia National Laboratories, Albuquerque, N.M., 1993.

14. Mandell, J.F., "Fatigue Behavior of Fibre-Resin Composites", Chapter 4, *Developments in Reinforced Plastics-2*, G. Pritchard Ed.

15. O'Brien, T.K., "An Evaluation of Stiffness Reduction as a damage Parameter and Criterion for Fatigue Failure in Composite Material," Ph.D. Dissertation, Virginia Polytechnic Institute and State University, October, 1978.

16. Williams, R. S., Fatigue Damage Mechanisms in Fiber Reinforced Composite Materials, PH.D. Dissertation, VPI & SU, 1975.

17. Daniel, M.M. and Lee, J.W., "Damage Development in Composite Laminates Under Monotonic Loading", *Journal of Composites Technology & Research*, Vol. 12, No. 2 pp. 98-102, 1990.

18. Hahn, H.T., and Kim, R.Y., "Fatigue Behavior of Composite Laminates," *Journal of Composites Materials*, Vol. 10, pp.156, 1976.

19. Davis, L.Wl, and Sullivan, P.G. "Nondestructive Evalution," *Summary of the Proceedings of the Second Conference on Carbon Fiber Reinforced Metal Matrix Composites*, Monterey, California, 1978.

20. Knott, M.A., and Stinchcomb, W.W., "Non-Destructive Evaluation of Fatigue Damage in Boron-Aluminum Composites with Initial Defects," *Proceedings of the 12th Symposium on Non-Destructive Evaluation*, Southwest Research, San Antonio, Texas, 1979.

21. Stalnaker, D.O. and Stinchcomb, W.W., "Load History-Edge Damage Studies in Two Quasi-Isotropic Graphite Epoxy Laminates", *Composite Materials: Testing and Design, ASTM STP 674*, American Society or Testing and Materials, pp. 620-641, 1979.

22. Yang, J.N., "Fatigue and Residual Strength Degradation for Graphite/Epoxy Composites under Tension-Compression Cyclic Loading", *Journal of Composite Materials*, Vol. 12, pp. 19-39, 1978.

23. Yang, J.N. and Du, S., "An Exploratory Study Into the Fatigue of Composites Under Spectrum Loading", *Journal of Composite Materials*, pp. 511-525, 1983.

24. Radhakrishnan, K., "Fatigue and Reliability Evaluation of Unnotched Carbon Epoxy Laminates", *Journal of Composite Materials*, Vol. 18, 1984.

25. Lee, J.W., Daniel, I.M., and Yaniv, G., "Fatigue Life Prediction of Cross-Ply Composite Laminates", *Composite Materials: Fatigue and Fracture, ASTM STP 1012*, Lagace, P.A. Ed., American Society for Testing and Materials, Philadelphia, pp. 1928, 1989.

26. Wang, S. S. and Chim, E. S.-M., "Fatigue Damage and Degradation in Random Short-Fiber SMC Composite," *Journal of Composite Materials*, Vol. 17, 1983, pp. 114-134.

27. Poursatip, A., Ashby, M. F. A., and Beaumoun, P. W. R., "The Fatigue Damage Mechanics of a Carbon Fibre Composite Laminates: I-Development of the Model," *Composites Science and Technology*, Vol. 25, 1986, pp. 193-218.

28. O'Brien, T.K. and Reifsnider, K.L., "Fatigue Damage Evaluation through Stiffness Measurements in Boron-Epoxy Laminates", *Journal of Composite Materials*, Vol. 15, pp.55-70, 1981.

29. Hwang, W. and Han, K.S., "Fatigue of Composites—Fatigue Modulus Concept and Life Prediction", *Journal of Composite Materials*, Vol. 20, 1986, pp. 154-165.

30. O'Brien, T.K., "Characterization of Delamination Onset and Growth in a Composite Laminate", *Damage in Composite Materials, ASTM STP 775*, American Society for Testing and Materials, Philadelphia, pp. 140-167, 1982.

31. Crossman, F.W. and Wang, A.S.D., "The Dependence of Transverse Cracking and Delamination on Ply Thickness in Graphite/Epoxy Laminates," in *Damage in Composite Materials, ASTM STP 775*, American Society for Testing and materials, Philadelphia, 1982, pp. 118-139.

32. Crossman, F.W., Warren, W.T., Wang, A.S.D., and Law, G.E., "Initiation and Growth of Transverse Cracks and Edge Delamination in Composite Laminates," *Journal of Composites*, Supplemental Volume, 1980, pp. 88-106.

33. Pagano, N.J. and Pipes, R.B., "Some Observations on the Interlaminar Strength of Composite Laminates", *International Journal of Mechanical Sciences*, pp. 679-688, 1973.

34. Wilkins, D.J., J.R. Eisenmann, R.A.Camin, W.S.Margolis and R.A.Benson, "Characterizing Delamination Growth in Graphite-Epoxy", *Damage in Composite Materials: Basic Mechanisms, Accumulation, Tolerance Characterization, ASTM STP 775*, American Society for Testing and Materials, pp. 168-183, 1982.

35. O'Brien, T.K., "Mixed-Mode Strain-Energy-Release Rate Effects on Edge Delamination of Composites," *Effects of Defects in Composite Materials, ASTM STP 836*, American Society for Testing and Materials, pp. 124-142, 1984.

36. Herakovich, C.T., "On the Relationship Between Engineering Properties and Delamination of Composite Materials," *Journal of Composite Materials*, Vol. 15, pp. 336-348, 1981.

37. Murthy, P.L.N. and Chamis, C.C., "Free-edge Delamination: Laminate Width and Loading Conditions Effects", *Journal of Composites Technology & Research*, Vol. 11, No. 1, pp. 15-22, 1989.

38. O'Brien, T.K., "Towards a Damage Tolerance Philosophy for Composite Materials and Structures," *Composite Materials: Testing and Design (Nineth Volume), ASTM STP 1059*, Garbo, S.P. Ed., American Society for Testing and Materials,

pp. 7-13, 1990.

39. Dexter, H.B. and Funk, J.G., "Impact Resistance and Interlaminar Fracture Toughness of Through-the-Thickness Reinforced Graphite/Epoxy," AIAA paper 86-1020-CP, 1986.

40. Mignery, L.A., Tan, T.M., and Sun, C.T., "The Use of Stitching to Suppress Delamination in Laminated Composites," *Delamination and Debonding of Materials, ASTM STP 876*, Johnson, W.S., Ed., American Society for Testing and Materials, Philadelphia, pp. 371-385, 1985.

41. Kim, R.Y., "Prevention of Free-Edge Delamination," *Proceedings of the 28th National ASMPE Symposium*, 1983.

42. Howard, W.E., Gossard, T., Jr., and Jones, R.M., "Reinforcement of Composite Laminate Free Edges with U-shaped Caps," AIAA Paper 80-0972, 1986.

43. Tan, S.C., "Characterization of Off-Axis Laminates Made by Folding", *Journal of Composite Materials*, Vol. 21, pp. 536-552, 1987.

44. Reed, R.M., "Long Term Fatigue of Glass Fiber Reinforced Composites Materials for Wind Turbine Blades", Master degree thesis, Montana State University, 1991.

45. Highsmith, A. L., "Edge Replication for Laminated Composites", Manual on Experimental Methods for Mechanical Testing of Composites, Society for Experimental Mechanics, Inc., Bethel, Connecticut, pp. 165-169, 1989.

46. Highsmith, A.L. and Reifsnider, K.L., "Stiffness-Reduction Mechanisms in Composite Laminates", *Damage in Comosite Materials, ASTM STP 775*, Reifsnider, K.L., Ed., American Society for Testing and Materials, pp. 103-117, 1982.

47. Shrininivas, M., "Three Dimensional Finite Element Analysis of Matrix Cracks In Multidirectional Composite Laminates, M.S. Thesis, Montana State University, 1993.

APPENDIXES

Table 1. Characteristic's and mechanical properties.

Material	Fiber Content (V_f%)	(0°) Fiber%[a]	(45°) Fiber%[b]	Edge Condition	Stitching Orientation	Elastic Modulus	Ultimate Tensile Strength
						(Msi)	(Ksi)
T	26.5	49.8	50.2	wrapped	0° and 45°		53
U	29.2	46.4	53.6	wrapped	90°		54
V	35	51	49	Unwrapped	90°	2.9	68
W	33.2	54	46	Unwrapped	0° and 45°	2.8	58

a: 0° fiber content as a percent of total fiber.

b: 45° fiber content as a percent of total fiber.

Table 2. Data of matrix crack density for Material W* .

Fatigue Loading								Static Loading	
Cycles	crack density (#/inch) $S_{max.}$ = 15000 psi			Cycles	crack density (#/inch) $S_{max.}$ = 12500 psi			Stress (psi)	(#/inch)
1	0	0	0	1	0	0	0	27000	2
10^3	1	0	3	10^3	1	0	0	33000	7
1×10^4	7	5	7	10^4	1	2	3	43000	14
8×10^4	9	8	10	10^5	3	3	5	50000	17
1.6×10^5	13	11	12	10^6	5	7	8	57000	18
2.4×10^5	16	14	19	2×10^6	10	13	16	60000	19
3.2×10^5	25	23	27	4×10^6	15	19	21	67500	19
3.6×10^5	27	26	27	6×10^6	20	23	22		
4.4×10^5	28	27	30	8×10^6	28	32	25		
4.6×10^5	28	27	30	10^7	32	34	35		
				1.2×10^7	34	36	38		
				1.4×10^7	36	37	39		
				1.58×10^7	36	37	39		

* The three data sets for fatigue crack density represent three separate test specimens, each measured over a two-inch gage length.

$S_{max.}$ = Maximum cyclic stress

MONTANA STATE UNIVERSITY LIBRARIES
3 1762 10220066 2

HOUCHEN
BINDERY LTD